4-26-2018

A study of albendazole and artemisinin drugs under electrochemical oxidation

Zahilis A. Mazzochette
Rowan University

A STUDY OF ALBENDAZOLE AND ARTEMISININ DRUGS UNDER ELECTROCHEMICAL OXIDATION

by

Zahilis A Mazzochette

A Thesis

Submitted to the
Department of Chemistry and Biochemistry
College of Science and Mathematics
In partial fulfillment of the requirement
For the degree of
Master of Science in Pharmaceutical Sciences
at
Rowan University
March 28, 2018

Thesis Chair: Amos Mugweru, Ph.D.

Dedication

I dedicate this thesis to my mother Edicta Castillo Perez for her unconditional support throughout my studies and always and to the loving memory of my late father, Jose Altagracia Perez. Thanks for being exceptional parents.

Acknowledgments

I would like to express my deepest gratitude to my research advisor Dr. Amos Mugweru for his guidance and for the invaluable research experience I gained in his lab. Thanks for the time you dedicated to teaching me electrochemistry and other methods of analysis. I wish to thank the members of my thesis committee Dr. Subash Jonnalagadda and Dr. Timothy Vaden for their advice on this research project and on career paths to follow this program. Also, thanks for being supportive and understanding.

Thanks to Rowan University Department of Chemistry and Biochemistry for the Teaching Fellowship position awarded to me during this program.

I also want to acknowledge my family for their encouragement, patience, and support throughout my educational journey.

Abstract

Zahilis Mazzochette
A STUDY OF ALBENDAZOLE AND ARTEMISININ DRUGS UNDER ELECTROCHEMICAL OXIDATION
2017-2018
Amos Mugweru, Ph.D.
Master of Science in Pharmaceutical Sciences

This work is aimed to investigate the metabolic behavior of albendazole and artemisinin. The electrochemical oxidation and reduction of these drugs were performed on electrode materials to mimic their metabolism in vivo using cyclic voltammetry and bulk electrolysis analysis. The oxidation of albendazole on gold electrode surface yielded albendazole sulfoxide and albendazole sulfone which are the main metabolites of this drug in vivo. Reduction of artemisinin on glassy carbon (GC) electrode surface yielded dihydroartemisinin and deoxy artemisinin. The formation of these products was monitored using liquid chromatography and mass spectrometry techniques. The redox processes for both drugs were shown to be irreversible and diffusion controlled. Bioactivation of artemisinin by hemoglobin was detected using a GC/carbon nanofibers (CNFs)/Hb biosensor. The catalytic effect of hemoglobin lowered the reduction potential of artemisinin by 475 mV. The apparent Michaelis-Menten constant (K_m) was 0.093 mM which shows excellent biological activity of the CNFs bound hemoglobin. Additionally, the biosensor showed a linear relationship with increasing artemisinin concentration. Therefore, it can be useful to determine concentration of this drug in solution and matrices such as biological fluids.

Table of Contents

Table of Contents (continued)

Table of Contents (continued)

List of Figures

Figure Page

List of Figures (continued)

List of Tables

Table Page

Chapter 1

An Introduction to Electrochemical Analysis of Pharmaceuticals

Electroanalysis of Pharmaceuticals

Application of electrochemical techniques to solve chemical problems started with the invention of polarography in 1922 by Jaroslav Heyrovsky, and the polarograph, one of the first automated analytical devices, by Heyrovsky and Shikata [1]. Heyrovsky's invention had a significant impact on the advancement of electroanalysis. He was awarded the Nobel Prize for chemistry in 1959 for this contribution [2]. Electroanalysis experienced its greatest advancement between the 1950s and 1970s with the development of new methods and instrumentation as well as interest in improving the electrode surfaces, which lead to the development of electrochemical sensors [1-2]. Electrochemical analysis has found applications in a wide variety of industries such as metal and pharmaceutical industries, as well as in research, environmental, and occupational health fields [3-4].

Electrochemical techniques have been utilized for the analysis of pharmaceuticals since the 1960s [5]. The interest in these techniques for drug analysis has increased remarkably since then. The increase in popularity can be attributed to the development of more sophisticated instrumentation and a better understanding of the techniques themselves [6]. Electrochemical techniques offer many advantages for the analysis of pharmaceuticals including excellent sensitivity at very low concentration, rapid analysis, small sample volumes, and easy sample preparation [5]. They offer excellent methods for concentration determination of drugs in pure solutions, dosage forms, and biological fluids. Additionally, electrochemical methods are very useful to obtain information about drugs' pharmacokinetics, mechanism of drug action, and electron transfer parameters [7].

Electrochemical Techniques Often used for Drug Analysis

Potentiometry, coulometry, and voltammetry are popular electrochemical techniques used for analysis of pharmaceuticals. Potentiometry methods measure the potential of a solution, between the working and reference electrodes, due to an applied controlled current. The difference in potential between the electrodes is used to determine the concentration of the analyte or analytes in solution. Coulometric titrations involve the generation of a chemical reactant at the electrode surface. Then, the generated reactant undergoes a chemical reaction with the analyte. Control potential coulometry is often referred to as bulk electrolysis. This technique will be described in more details later in this chapter as it was used in drug oxidation. Voltammetric methods are based on the application of a constant or varying potential at the surface of a working electrode and measuring the resulting current. The potential or voltage applied at the working electrode's surface serves as the driving force to carry out reduction or oxidation reactions [8]. In voltammetry, the applied potential is the controlled parameter, and it can be adjusted according to the reductive or oxidative properties of the drug species being analyzed. Two different waveforms can be obtained using voltammetry a time-voltage, and a current-voltage plot. A potential versus time waveform is obtained when a varying voltage is applied over a period of time. The second plot is obtained by applying a potential and measuring the current produced. The resulting curve is called a voltammogram from which information about the electrochemical properties of the species being analyzed can be obtained [8]. Voltammetry is very popular for the analysis of drugs and pharmaceuticals [4]. The choice of voltammetric method depends on the type of analyte and parameters to be determined. Table 1 shows different types of voltammetric

methods that have been used for the analysis of pharmaceuticals. In this work, cyclic voltammetry, amperometry, and bulk electrolysis are the electroanalytical methods used to study the redox behavior of albendazole and artemisinin. Therefore, a detailed discussion of these methods is offered.

Table 1

Voltammetric methods used for quantification, mode of action, and kinetic studies of pharmaceuticals.

Method	Drug	Type of Study	References
Cyclic Voltammetry (CV)	Cephalexin, Daunomycin, Dopamine Acetaminophen Chloroquine	Quantification, Mechanism of action, Electrochemical behavior, Kinetics	9-13
Square wave Voltammetry (SWV)	Nitrofurantoin, Riboflavin, Doxazosin Nandrolone Ceftazidime	Quantification, Electrochemical behavior	14-19
Anodic Stripping Voltammetry (ASV)	Dopamine, Doxazosin	Quantification	14, 16
Cathodic Striping Voltammetry (CSV)	Chlordiazepoxide Norfloxacine, Enoxacine	Quantification, Electrochemical behavior	20-21
Adsorptive Stripping Square Wave Voltammetry (AdSSWV)	Carvedilol, Levofloxacin Metoclopramide	Electrochemical behavior, quantification	22-24
Differential Pulse Voltammetry (DPV)	Nandrolone, Bergenin, Trimebutine, Ceftazidime	Electrochemical behavior, quantification	15, 17 25-26
Differential Pulse Polarography (DPP)	Artemether, Ciclopirox olamine	Quantification	27-28
Amperometry	Isoniazid, Ascorbic acid Sodium metabisulfite	Electrochemical behavior, quantification	29-31
Adsorptive Striping Voltammetry (ASV)	Ofloxacin, Fluoroquinolones	Quantification	32

Cyclic voltammetry. Cyclic voltammetry (CV) is a versatile analytical technique widely used in many areas of electroanalytical chemistry [4]. CV is especially popular for the analysis of drugs and pharmaceutical. In fact, it is among the first experiments carried out on drugs that are electro-active [33]. Cyclic voltammetry can be used to determine concentration of analytes, and it is especially useful for the study of redox reactions and homogeneous chemical reactions coupled to electron transfer processes [34]. During a CV experiment, the potential of the working electrode is ramped linearly versus time. The voltage applied to the working electrode is increased from an initial value $E_{initial}$ to a predetermined limit, E_{limit} (the switching potential). At this point, the direction of the scan is reversed completing one full cycle. The scanning can be stopped at this point, or a series of cycles between $E_{initial}$ and E_{limit} can be performed. Repeated scanning is very useful to probe the stability of modified working electrodes [35]. Furthermore, changes that appear on repetitive scans can reveal information about reaction mechanisms [8].

Amperometry. Amperometry is classified as a voltammetric method. In amperometry, a constant reducing, or oxidizing potential is applied, and the resulting steady-state current is usually measured as a function of time [36]. The magnitude of the resulting current correlates with the concentration of the oxidized or reduced analyte. Therefore, this technique is reliable and efficient to determine the concentration of one or numerous electroactive substances in solution by selectively choosing the magnitude of the applied potential and electrode material [36]. Amperometry is also widely used for the analysis of electrochemical sensors and biosensors [36].

Bulk electrolysis. Control potential coulometry is referred to as bulk electrolysis. With this technique, a constant potential is applied to oxidize or reduce the substance of interest completely. A large working electrode with a surface area about one hundred times larger than a standard electrode is used to speed up the electrochemical conversion. The experiments are carried out under stirring conditions to aid transport of electroactive material to the electrode surface. "In controlled potential coulometry, the potential of the working electrode is maintained at a constant level such that the analyte conducts charge across the electrode-solution interface. The charge required to convert the analyte to its reaction products is then determined by integrating the current-versus-time curve during the electrolysis" [37]. The amount of charge measured during the experiment is used to determine the concentration of analyte in solution. Therefore, controlled potential coulometry is a very valuable technique for quantitative analysis [38]. This technique can be used for synthetic purposes as long as the product is neutral and can be isolated from the electrolyte solution. If the products cannot be isolated, then analytical techniques such as UV-Vis, NMR, HPLC, and mass spectrometry (MS) can be utilized to analyze them in solution [38]. In this work, bulk electrolysis was used to completely electrolyzed samples of albendazole and artemisinin. The electrolysis products were analyzed using HPLC-MS.

The Electrochemical Cell

Most electrochemical analysis of pharmaceuticals takes place in a three-electrode electrochemical cell which consists of a working electrode, an auxiliary or counter electrode, a reference electrode, and a supporting electrolyte. Redox reactions take place on the surface of the working electrode. The choice of working electrode depends on the nature of the analyte and the type of analysis to be performed. For example, cyclic

voltammetry is performed using working electrodes with a small surface area such as a standard gold, glassy carbon or platinum electrode (Figure 1a) while bulk electrolysis can be performed efficiently and rapidly by using a working electrode with a large surface area (Figure 1b). Standard working electrodes are mostly covered with insulating material just leaving a carefully controlled circular area exposed (about 1mm wide) where the reaction takes place. The auxiliary electrode is usually a platinum electrode, and it is needed to complete the circuit along with the working electrode. The reference electrode is used to measure the applied potential and does not pass any current. A supportive electrolyte is used to avoid migration of the species of interest through the solution. In some experiments, the supportive electrolyte can be used as a solvent.

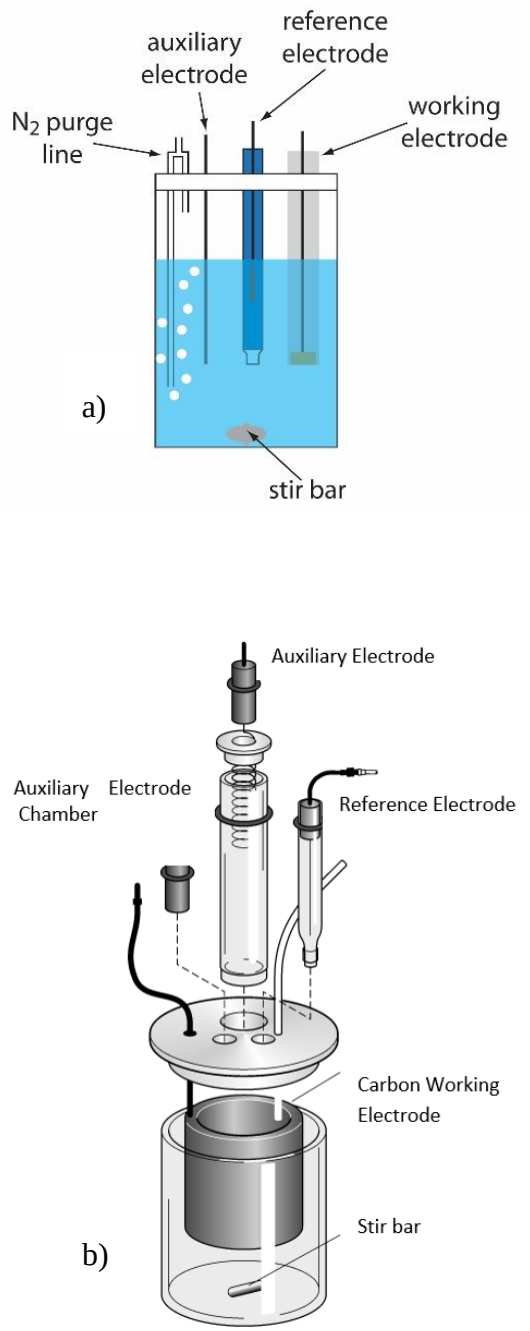

Figure 1. Electrochemical cells: a) a typical voltammetry cell. b) Bulk electrolysis cell, featuring a large carbon working electrode.

Research Objective

Understanding the electrochemical behavior of pharmacologically active molecules is of high importance since metabolic pathways of these molecules undergo redox transformations [39]. Due to the similarities between biological and electrochemical reactions, it can be assumed that redox mechanisms taking place at the electrode surface and inside the body happen through similar processes. Therefore, the redox properties of drug molecules can give us insight into their metabolic fate and pharmacological activity in vivo [33]. This study is aimed to use chromatographic and electroanalytical techniques to elucidate mechanistic parameters from the redox reactions of albendazole and artemisinin. Both albendazole and artemisinin have been reported as potential anticancer agents [40-41]. A clear understanding of the electron transfer processes of these drugs is fundamental to better understand their anticancer properties and for the development of more potent analogs.

Chapter 2

Electrochemical Oxidation of Albendazole

Introduction

Albendazole (ABZ) is a broad spectrum benzimidazole carbamate used for the treatment of helminths and diseases such as neurocysticercosis, strongyloidiasis, and microsporidiosis caused by such parasites [42-43]. Albendazole has been in use for about 40 years in humans and animals with few side effects among them mild gastrointestinal discomfort, dizziness, and rash [44]. ABZ is a prodrug which is oxidized by liver enzymes and transformed into albendazole sulphoxide (ASOX) its pharmacologically active metabolite. Albendazole sulphoxide is further oxidized into albendazole sulphone (ASON) an inactive metabolite [44-45] (Figure 2). Albendazole works by selectively binding to parasites' ß-tubulin preventing the formation of microtubules and stopping cell division. It also impairs glucose uptake leading to energy depletion and parasite death [46-47]. Albendazole's solubility in aqueous solution is very poor due to the nature of its molecular structure hence high concentration of this drug is administered to improve absorption and achieve therapeutic levels [48-49]. Pharmacokinetics of albendazole have been studied in both human and animals. The rate of absorption of albendazole was found to be erratic and varies greatly between individuals and animal species [49-50]. There is continued interest in the study of albendazole's properties and metabolism. In fact, there has been extensive research in developing attractive and fast methods for studying ABZ and its metabolites. Several reported analytical techniques for the analysis of albendazole include ultrahigh performance LC coupled with a mass spectroscopy detector, high-performance liquid chromatographic (HPLC) [51-53], solid phase extraction coupled with

HPLC, and electrochemical studies [54-55]. In this chapter, the electrochemical oxidation of albendazole is carried out to elucidate significant kinetic parameters helpful for further understanding of its metabolic fate.

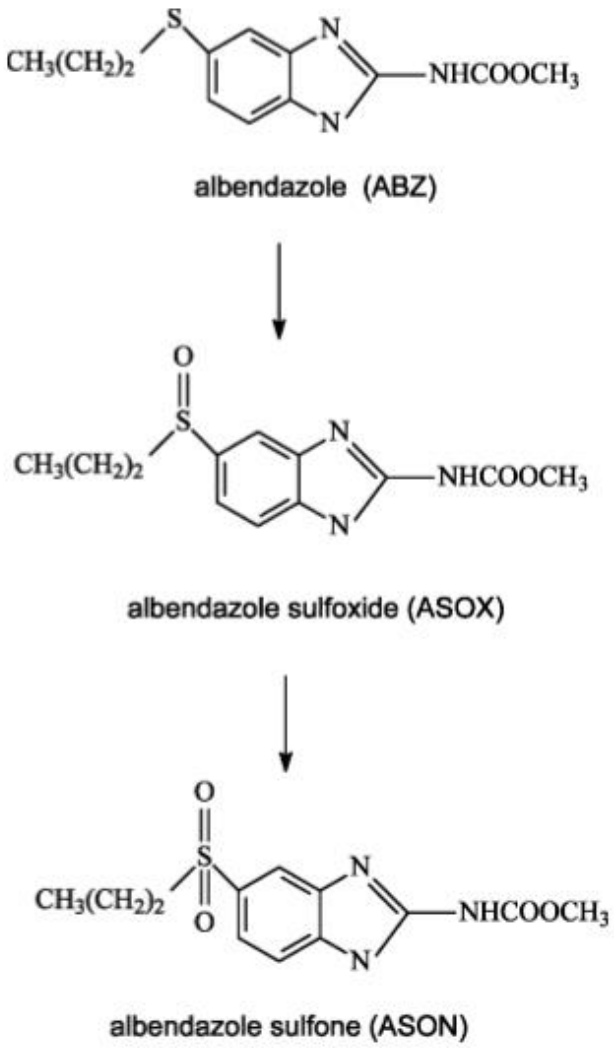

Figure 2. Albendazole and its metabolites: Albendazole sulphoxide and albendazole sulphone [39].

Experimental Methods

Chemicals. Albendazole was purchased from Sigma Aldrich. Tetrabutyl ammonium bromide (TBAB) was purchased from WWR (West Chester, PA). A (7.55×10^{-3} M) albendazole solution in acetonitrile containing (0.05M) TBAB as the supporting electrolyte was used for this study. All analytical reagents were used as received. DI water was used for all other applications. All chemicals were of analytical grade or HPLC grade.

Electrochemical apparatus. Cyclic voltammetry (CV) and amperometric studies were carried out with a computer controlled electrochemical workstation (CHI 660c, USA) with an ohmic drop (IR) 98% compensated. A three-electrode electrochemical cell with a glassy carbon working electrode, a platinum wire as a counter electrode, and a Ag/AgCl as the reference electrode were used for all electrochemical experiments. The Ag/AgCl reference electrode was equipped with a glass tip, separated from the sample solution compartment by a salt-bridge containing KCl and terminating in a medium porosity glass frit. Cell resistance, IR, as measured by the CH Instruments, was 98% compensated in all voltammetric experiments. All work was done at the ambient temperature of the laboratory (23℃).

Electrode surface preparation procedure. The glassy carbon working electrode (0.07 cm^2) and the platinum wire counter electrode were obtained from Bioanalytical Systems Inc. (West Lafayette, IN). Glassy carbon electrodes require polishing in alumina (0.1 μm particle sizes) and rinsing thoroughly in pure water and finally ultra-sonicated in the same media before use. Prior to this study, glassy carbon electrodes were initially polished on one μm diamond polishing paste then ultrasonicated in ethanol and distilled

water successively for 1 minute, followed by rinsing in pure water and then dried in air. This step was then followed by alumina polishing and thorough rinsing, as indicated above.

Chromatographic procedure. The HPLC-UV analysis was carried out using an Agilent 1100 series HPLC unit. The UV detector was set at 254 nm wavelength. Separations were carried on a ZORBAX XDB-CN column (4.6 mm × 150 mm long and five μm particle size, Agilent Technologies). A Zorbax CN guard column (4.6 mm cartridge, Agilent Technologies) was used to preserve the analytical column. The mobile phase consisted of acetonitrile methanol and DI water (59:27:14). The chromatographic run was performed at a flow rate of 1 mL/min.

Mass spectrometry procedure. The mass spectrometer was a Micromass Quattro micro unit. It was set to ESI in positive ion mode. The settings of the mass spectrometer were as follows: the desolvation gas (N2) and flow were operated at 500 ℃ and 5 L/min, respectively. The corona was operated at 2 μA while the cone voltage was set at 25 V. The extractor lens was at 5 V while the RF lens was at 0.2 V. The mass spectrometry collision gas was an N2 of high purity (>99.9995).

Results and Discussion

Voltammetric oxidation of albendazole. The electrochemical oxidation of ABZ was studied on a glassy carbon electrode surface using cyclic voltammetry. The cyclic voltammogram of 7.55×10^{-3} M albendazole solution in acetonitrile was recorded at a potential window from 0 V to 2.0 V versus Ag/AgCl reference electrode. The voltammogram shows two broad anodic peaks (Figure 3).

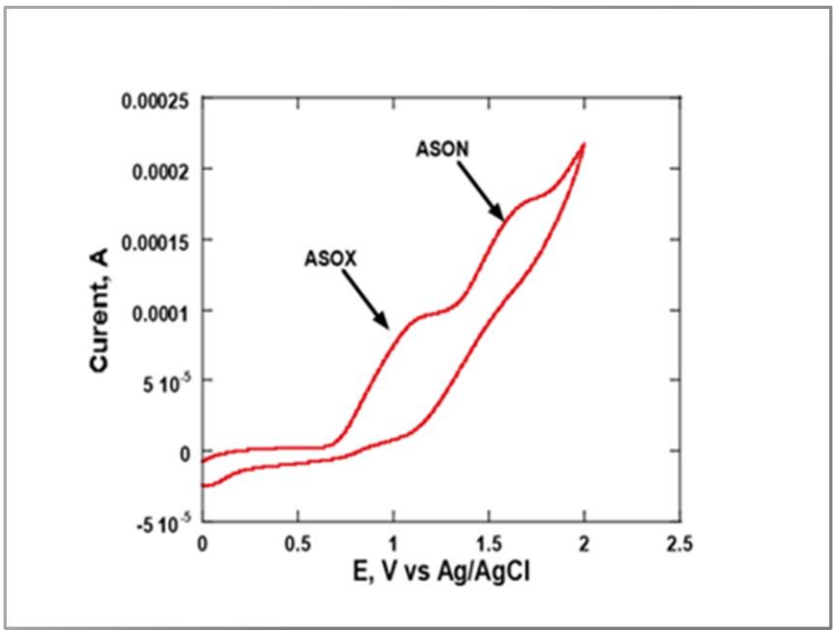

Figure 3. Cyclic voltammogram of (7.55×10^{-3} M) ABZ in acetonitrile containing 0.05M TBAB solution. CV was performed using a glassy carbon electrode at 30 mV/s scan rate.

The first peak was at about 1.2 V versus Ag/AgCl reference electrode and the second peak occurred at about 1.6 V. During the reverse scan, no reduction peak corresponding to the anodic response was observed which indicates that the oxidation of albendazole is an irreversible process [39, 56]. In a reversible process, a cathodic or reduction peak of about the same magnitude of the anodic peak is formed during the reverse scan and vice versa. The reversibility or irreversibility of an electrochemical reaction provides significant information about the rate at which the electron transfer occurs between the working electrode and the redox species in solution. Reversible reactions occur quickly without significant thermodynamic barriers. If the electron transfer is not fast enough and the electrochemically generated species is not stable, the unstable species undergoes a chemical reaction rendering the system irreversible [56]. Cyclic voltammetry is an effective technique for detecting the formation of reaction intermediates as in the case of ABZ.

Oxidation of ABZ at the electrode surface leads to the formation of albendazole sulfoxide which undergoes further oxidation and transformed into albendazole sulfone [45]. The first and second peak waves in figure 3 were later confirmed using LC-MS to be due to the formation of albendazole sulfoxide and albendazole sulfone respectively. The measured peak current of the first peak wave was found to increase with the scan rate while the second peak also increased accordingly but disappeared at scan rates higher than 100 mV/S. The disappearance of the second peak indicates that ASON did not form at scan rates higher than 100 mV/S.

The scan rate analysis indicates that the oxidation of albendazole is controlled by diffusion. Diffusion of analyte towards the electrode occurs when there is a concentration difference between the electrode surface and the bulk solution. As species are reduced or oxidized at the electrode surface, a concentration gradient is formed. Molecules move from areas of greater concentration to areas of lesser concentration [37] at a rate dictated by the concentration gradient. A plot of peak current versus the square root of scan rate ($v^{1/2}$) produced a linear relationship (Figure 4a), suggesting a diffusion-controlled electrode process according to the accepted theory [57-58]**.** Increasing the scan rates also increases the potential at the electrode surface. As a result, the concentration of analyte at the electrode surface becomes smaller, and diffusion towards the electrode surface increases [37]. The peak potential (E_p) of the anodic peaks were also dependent on the scan rate. E_p shifted to more positive potentials on increasing the scan rate. A linear relationship between the peak potential and log (scan rate) was obtained (Figure 4b). Such linearity confirms the irreversible nature of the electro-oxidation of albendazole [59].

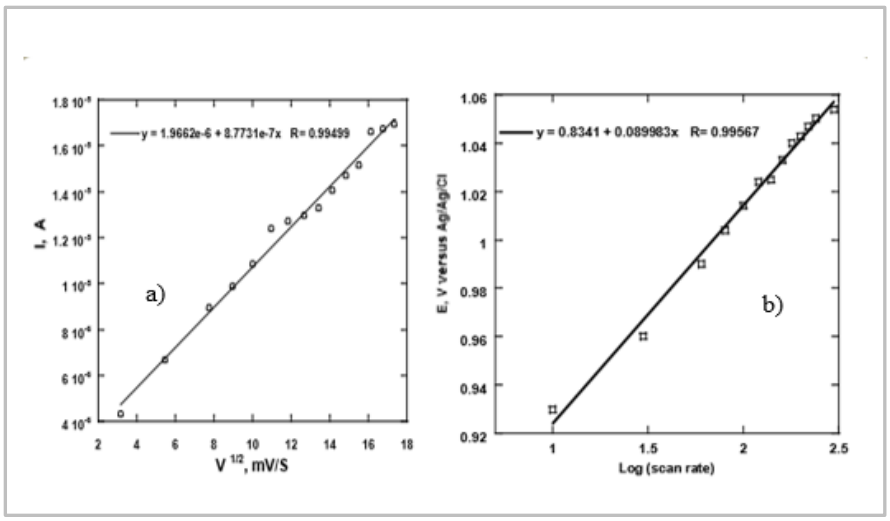

Figure 4. Albendazole (7.55×10^{-3} M) in acetonitrile showing peak currents and peak potentials: (a) Peak currents versus square root of scan rate; (b) Peak potentials with log of scan rate for peak wave at 1.2 V versus Ag/AgCl electrode.

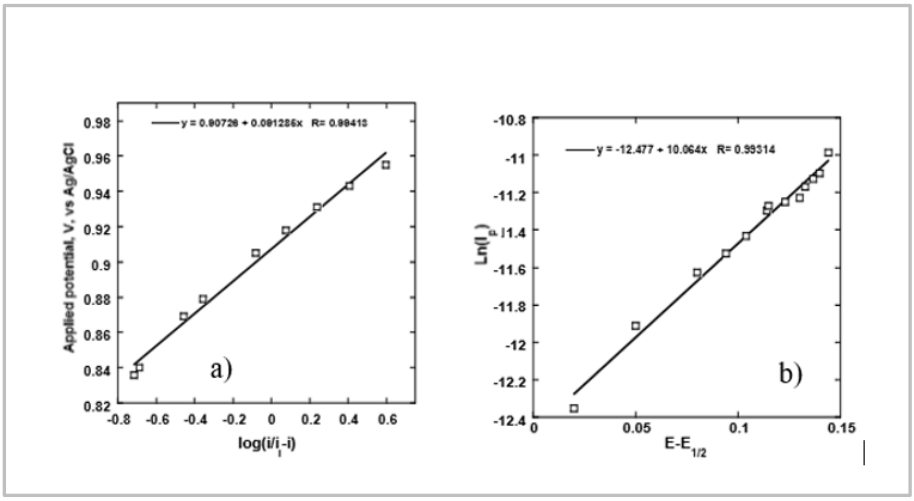

Figure 5. Applied potential vs. log $\left(\frac{i}{i_l - i}\right)$ at a scan rate of 100 mV/s; (b) Measured current (Ln (i_p) versus ($E-E_{1/2}$) at a scan rate of 100 mV/s for (7.55×10^{-3} M) albendazole in acetonitrile containing 0.05M TBAB at a glassy carbon electrode.

Kinetic parameters for albendazole's oxidation were estimated using experimental data obtained from figure 5 above together with equations 1, 2, and 3.

$$E = E_{1/2} - \frac{RT}{\alpha nF}\log\left(\frac{i}{i_l - i}\right) \qquad \text{Equation 1}$$

$$i_p = 0.227\,nFAC_0K_h e^{\frac{\alpha n_a F}{RT}}\left(E - E_{1/2}\right) \qquad \text{Equation 2}$$

$$Ln\left(i_p\right) = Ln\left(0.227\,nFAC_0K_h\right) - \frac{\alpha n_a F}{RT}\left(E - E_{1/2}\right) \qquad \text{Equation 3}$$

Where i is the current at any measured potential and i_l is the limiting current, α is the coefficient of electron transfer, n is the number of electrons transferred, $E_{1/2}$ is the mid-point potential, E is the applied potential, T is the temperature in Kelvin (298), R is the gas law constant (8.314), F (Faraday constant = 96480), k_h is the heterogeneous rate constant, A is the area of the electrode surface, and C_0 the initial analyte concentration. A plot of E versus log $\left(\frac{i}{i_l - i}\right)$ (Figure 5a) gives a straight line which slope and y-intercept relate to the charge transfer characteristics. The y-intercept corresponds to the value of $E_{1/2}$ which according to Figure 5a was found to be 0.91V versus Ag/AgCl. The plot of Ln i_p versus (E-$E_{1/2}$) (Figure 5b) also gave a straight line whose y-intercept and slope provide information to calculate the heterogeneous rate constant and electron transfer coefficient using equation 5. For an irreversible system, α is assumed to be 0.5 [60].

Hence the number of electrons transferred in the electro-oxidation of ABZ to ASOX was calculated as 1.3 ≈1. The value of K_h was calculated to be about 1.39×10^4 S^{-1} cm^2. The average current density at 100 mV/s was about 214 µA/ cm^2 which also supports the diffusion-controlled mass transport of albendazole towards the electrode surface.

Figure 6a shows the plot of peak current versus scan rates for the second peak wave obtained during the electro-oxidation of ABZ. This peak was only observed at scan rate lower than 100 mV/s and potentials higher than 1.5 V versus Ag/AgCl electrode. A linear relationship between peak current and the square root of scan rates was obtained for the second peaks as well (Figure 6b). Like the conversion of ABZ to ASOX, this indicates that the electron transfer reaction for the conversion of ASOX to AZON is diffusion controlled.

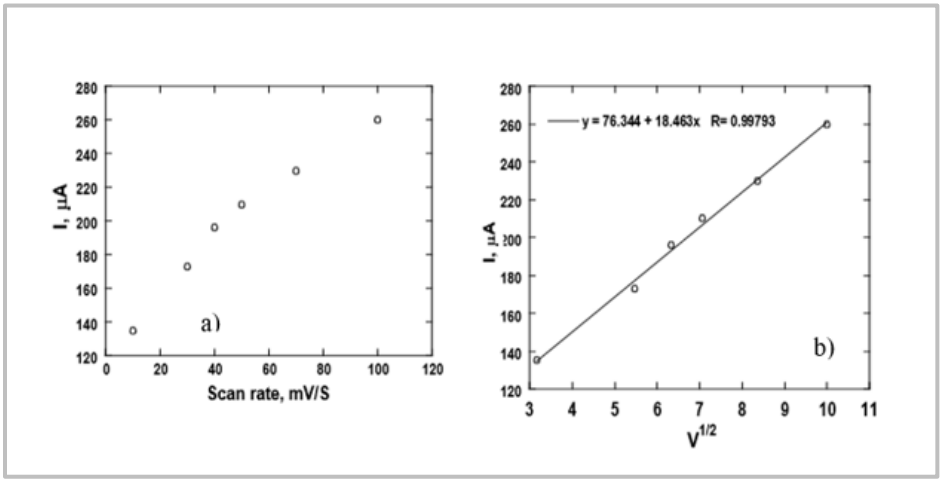

Figure 6. Variation of peak current for (7.55×10^{-3} M) albendazole for second peak wave: a) with scan rate b) with square root of scan rate at glassy carbon electrode.

A plot of E_p versus scan rate was obtained under the same scan rate values (Figure 7a). The relationship between the peak potential and log ν was linear (Figure 7b) with a correlation coefficient of 0.990. Such behavior reveals the irreversible nature of the electrochemical oxidation of ASOX to ASON.

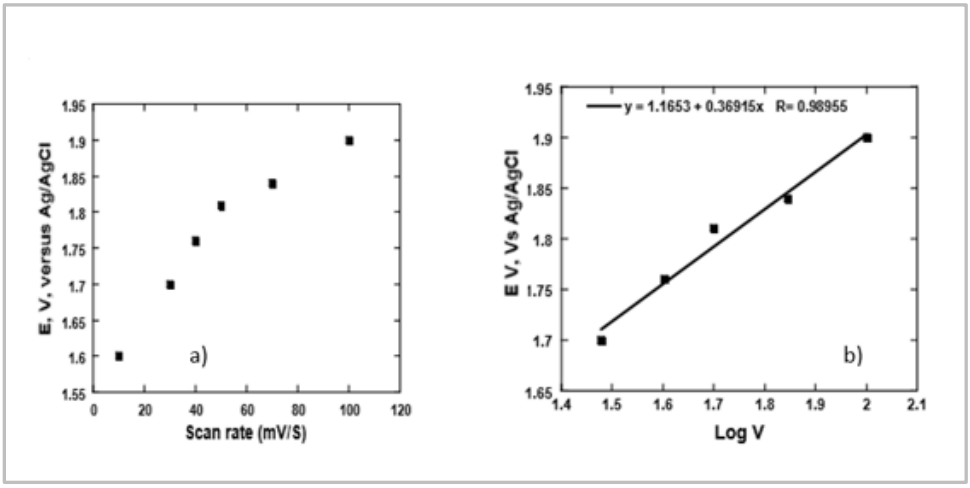

Figure 7. Variation of peak potential for (7.55 x 10^{-3} M) albendazole for second peak wave: a) with scan rate b) at glassy carbon electrode.

Bulk electrolysis analysis. The electrolysis of albendazole (7.5 x 10^{-3} M) in a 59:27:14 mixture of acetonitrile, methanol, and deionized water solution was carried out using a glassy carbon electrode. The purpose of bulk electrolysis is to completely oxidize or reduce the analyte in solution. During bulk electrolysis, the solution is constantly stirred to maintain a continuous flow of fresh solution in the vicinity of the electrode surface. This type of mass transport is called forced convection, and it is the simplest way of transferring the electroactive species to the electrode surface [37]. The electro-oxidation

of albendazole was investigated as a function of time at two different potentials (1.5 V and 1.7 V). First, the electrode potential was fixed at 1.5 V versus Ag/AgCl for six hours. 1 ml of the electrolyzed solution was drawn out every hour using a syringe and filtered using a 0.45 nm filter. The same procedure was carried out at 1.7 V. The solutions were analyzed using HPLC and mass spectrometry.

Chromatographic analysis. Figure 8a shows the chromatograms of ABZ before and after 1-5 hours of electrolysis. The peaks at about 1.9 minutes correspond to unreacted ABZ molecules with the highest peak corresponding to albendazole solution before electrolysis. After one hour of electrolysis, a chromatographic peak appeared at about 1.7 minutes and another smaller peak at about 1.5 minutes. These peaks can be attributed to the oxidation products of albendazole. The peak at 1.7 minutes increased remarkably as the electrolysis continued while the smaller peak was saturated after three hours of electrolysis. The peak due to albendazole (peak at 1.9 min.) decreased as the electrolysis proceeded indicating its consumption as the products were formed. Figure 8b illustrates the reactant and products profile as a function of electrolysis time.

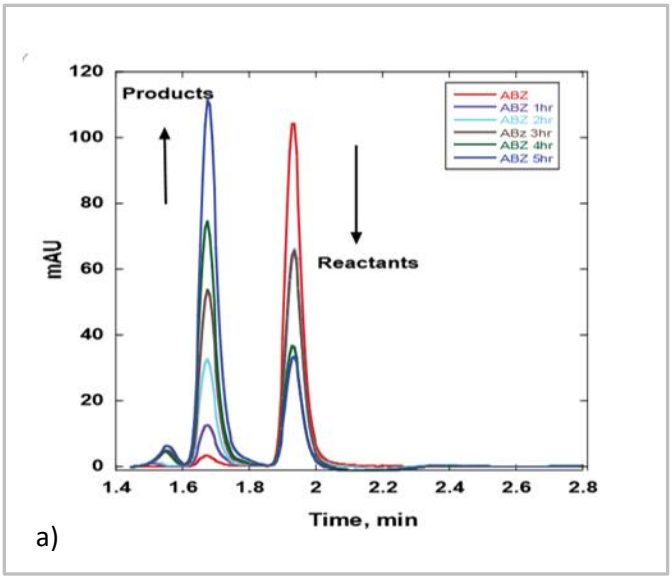

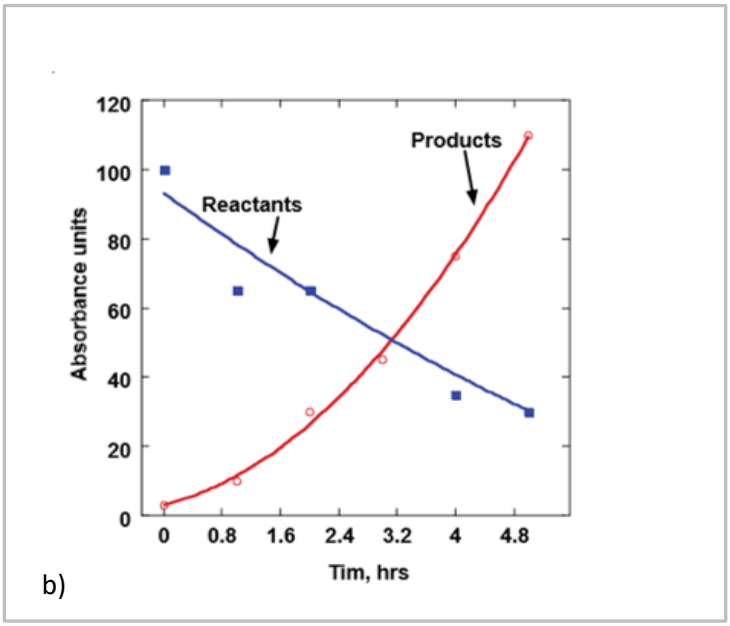

Figure 8. Chromatographic analysis of electrolyzed solution of ABZ: a) sampled at different times using UV detector at 254 nm and electrolyzed at 1.5 V versus Ag/AgCl electrode and b) reactant and products profile measured as a function of time using the chromatographic results obtained from the electrolysis of albendazole.

Increasing the voltage of electrolysis from 1.5 V to 1.7 V resulted in the formation of another chromatographic peak at 2.5 minutes and disappearance of the peak at 1.5 minutes (Figure 9). This new peak can be correlated to the anodic peak at about 1.6 V obtained on the CV of albendazole (Figure 3). Both peaks are likely due to the formation of albendazole sulfone.

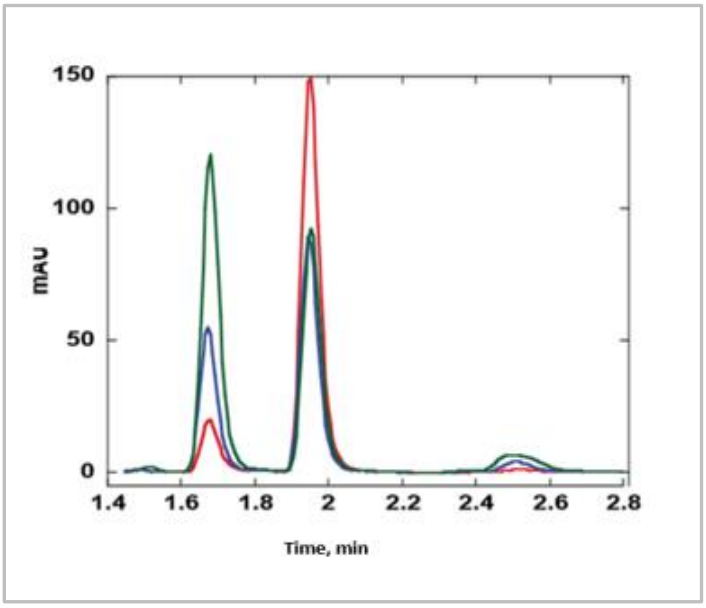

Figure 9. Chromatographic analysis of ABZ solution electrolyzed at 1.7 V versus Ag/AgCl electrode, sampled at different times using UV detector at 254 nm.

Further characterization of the electro-oxidation products of albendazole was carried out with an LC-MS Instrument using the same column and mobile phase flow rates as above. Figure 10 shows a mass spectrum of the initial ABZ peak obtained at 1.9 minutes. The initial drug, labeled A in the figure has well-known fragments with m/z of

the molecular ion at 266, other fragments with m/z 234, 191, correspond to structures B and C. Wu et al. [55] also observed these fragments during MS analysis of albendazole.

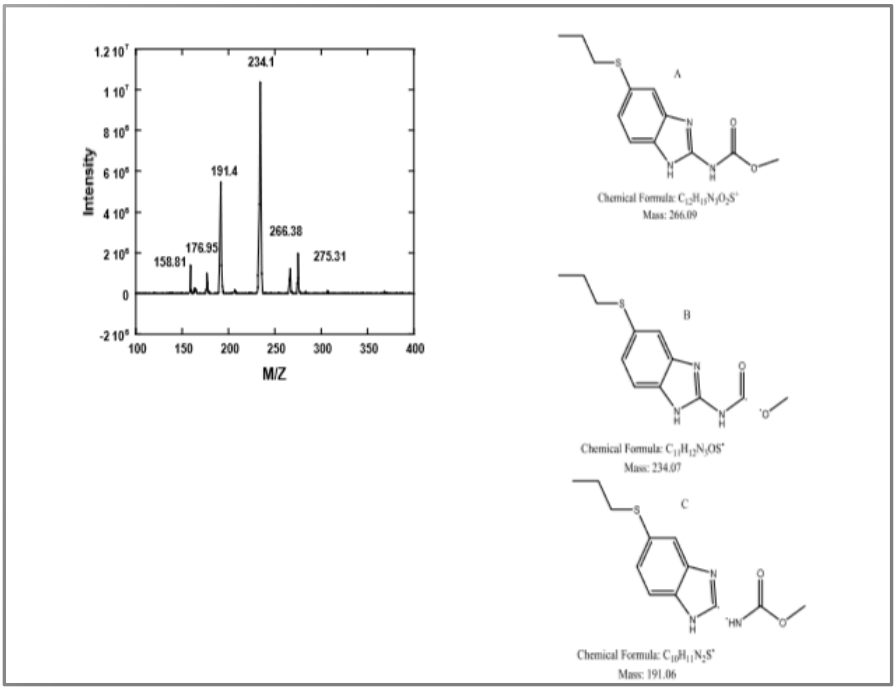

Figure 10. Mass spectrum of albendazole before electrolysis. Chromatographic peak at 1.9 minutes.

Figure 11 shows the mass spectra for the chromatographic peak at 1.7 minutes. This peak is likely due to the formation of albendazole sulfoxide since it experienced steady increase with time of electrolysis. The fragment with m/z 282 (D in figure 11) can be attributed to the molecular ion of ASOX. Fragments with m/z of 207 and 239 are given as E and F.

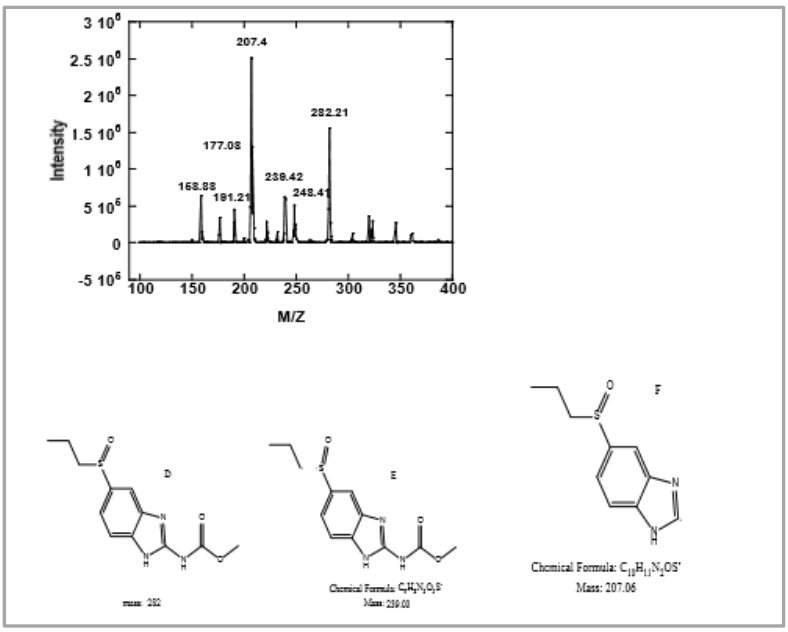

Figure 11. Mass spectrum of albendazole after electrolysis. Chromatographic peak at 1.7 minutes.

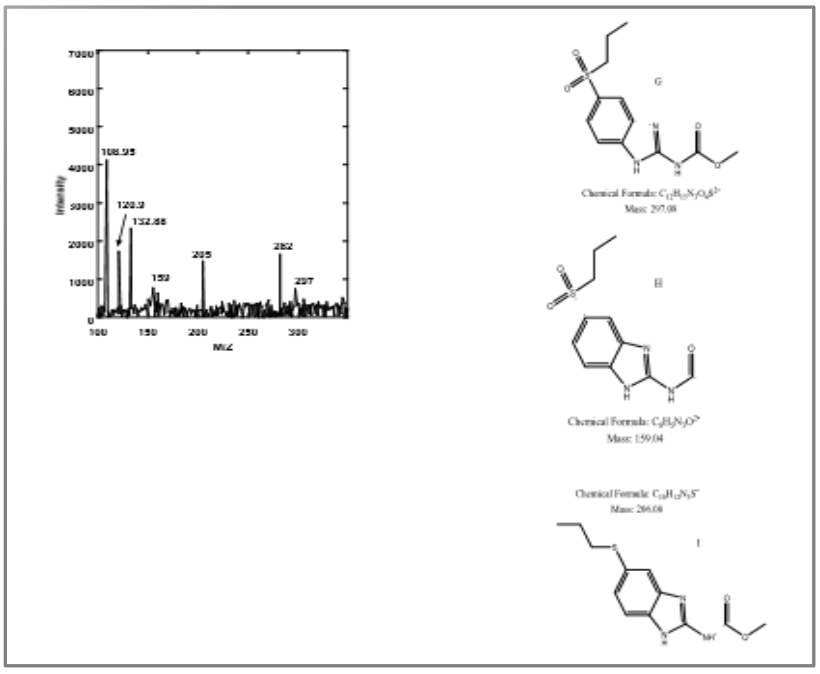

Figure 12. Mass spectrum of albendazole after 4 hours of electrolysis. Chromatographic peak at 2.5 minutes.

Figure 12 shows the mass spectra of the chromatographic peak at 2.5 minutes. This peak is thought to represent the formation of albendazole sulphone on the electrode surface. The molecular ion peak of albendazole sulphone is likely to be m/z 297. Other fragments obtained such as m/z of 159, 206, and 108.95 could not be accounted for.

Conclusion

The electrochemical oxidation of albendazole on glassy carbon electrode surface followed and ECE (multiple electron transfer with intervening chemical reaction) mechanism. Two electrons are transferred during the electrode process although not in a concerted fashion. The first step involves oxidation of albendazole followed by a chemical reaction and formation of albendazole sulfoxide. In the second step, ASOX is oxidized with subsequent formation of albendazole sulfone. The electrode reaction was therefore irreversible and limited by diffusion-controlled mass transfer. αn was calculated to be 0.652 and K_h was approximately 1.39×10^4 S^{-1} cm^2. Bulk electrolysis followed by HPLC analysis confirmed the generation of two electrolysis products. The products eluded at 1.7 and 2.5 minutes (Figures 14) can be attributed to the formation of albendazole sulfoxide and albendazole sulfone respectively. Mass spectra of the electrolyzed solution of albendazole reveal peaks at m/z 282 and m/z 297 that can be representative of the molecular ions of ASOX and ASON. These results further support the formation of these products during electrolysis.

Chapter 3

Electrochemical Reduction of Albendazole on Gold Electrode Surface

Introduction

The efficacy of albendazole has been well established for the treatment of helminths and related diseases [43] in spite of its low aqueous solubility. Albendazole is administered orally and in high dosages in order to achieve therapeutic concentrations [61]. There has been increased interest in the study of albendazole's aqueous solubility [62-65] to improve the formulation process for oral administration as well as for development of systemic formulations. Various studies have shown that albendazole has promising anticancer properties against various types of cancer tumors, i.e., colorectal, pancreatic, ovarian, breast, and prostate cancer [66-67]. However ever, because of its poor solubility, albendazole cannot be administered intravenously. None or very little of this drug reaches the systemic circulation when administered orally due to erratic absorption and extensive first-pass metabolism [64]. Therefore, continued research on albendazole is essential. Voltammetric techniques have been shown very effective for kinetics and metabolic studies of pharmaceutical compounds. Chapter 2 of this work focuses on the electrochemical oxidative behavior of albendazole. In this chapter, its reductive behavior on gold electrode surface is investigated.

Experimental Methods

Chemicals. Acetonitrile, methanol, Tetrabutylammonium bromide (TBAB) were purchased from WWR (West Chester, PA). Albendazole was purchased from Sigma Aldrich. The albendazole solution was prepared in a 1:1 ratio of acetonitrile/methanol as

the solvent containing (TBAB). The TBAB was used as the supporting electrolyte. All other chemicals were HPLC grade.

Electrochemical apparatus. Electrochemistry was carried out with a computer controlled electrochemical workstation (CHI 660c, USA) with 99%ohmic drop or IR compensation. A gold electrode was used as the working electrode, a platinum wire as the counter electrode, and a Ag/AgCl reference electrode were used for all electrochemical experiments. The Ag/AgCl was equipped with a glass tip, separated from the sample solution compartment by a salt-bridge containing KCl and terminating in a medium porosity glass frit. All electrochemical measurements were carried out under ambient conditions.

Electrode surface preparation. The gold working electrode (0.01 cm^2) and the platinum wire counter electrodes were obtained from Bioanalytical Systems Inc. (West Lafayette, IN). The gold electrode was polished using alumina (0.1 mm particle size) and rinsed thoroughly in pure water and finally ultra-sonicated in methanol for 1minute, followed by rinsing in pure water and then dried in air.

Bulk electrolysis procedure. The bulk electrolysis reduction of albendazole was carried out in tetrabutylammonium bromide-acetonitrile solution under stirring conditions for 7 hours. The potential of the reaction was fixed at 1.5 V versus Ag/ AgCl. 100 mL aliquots of the reaction mixture were withdrawn every hour. The solution reaction mixtures were diluted with mobile phase, filtered and analyzed using chromatographic techniques.

HPLC procedure. The chromatographic analysis was carried out using an Agilent 1100 series HPLC unit. The detector was a UV-Visible with the wavelength set at 254 nm. Separations were carried out at room temperature on a C-18 column ZORBAX 300SB (4.6X150 mm long and with 3.5 mm particle size, Agilent Technologies). The mobile phase consisted of acetonitrile, methanol and de-ionized water (59:27:14). The chromatographic run was performed under isocratic conditions at the flow rate of 1mL/min.

Mass spectrometry procedure. The mass spectrometry analysis was performed using a Micromass Quattro micro API Mass Spectrometer. The MS was set to ESI in positive ion mode. The settings of the mass spectrometer were as follows: the de-solvation gas (N2) and flow were operated at 1988Cand 249 L/hour respectively. The corona was operated at 2 mA, while the cone voltage was set at 60 V. The extractor lens was at 3Vwhile the RF lens was set at 0.0 V. The mass spectrometry collision gas was an N2 of high purity (>99.9995).

Results and Discussion

Voltammetric reduction of albendazole. Reduction of albendazole was investigated on gold electrode surface using cyclic voltammetry. A 0.05 M TBAB solution was used as the supporting electrolyte to avoid electrolytic migration of ABZ molecules as the potential is applied. The reduction was carried out at a potential window of 1.0 V to -1.6 V versus Ag/AgCl electrode. The recorded cyclic voltammogram shows three well-defined reduction peaks (Figure 13). The first peak was at about -1.0 V versus Ag/AgCl reference electrode, the second peak occurred at around -0.6 V, and the third peak was registered at +0.1 V. During the reverse scan, no oxidation peaks corresponding

to the reduction peaks were observed. This suggests that the reduction of albendazole is irreversible. As previously mentioned, in a reversible process, the reverse scan forms a cathodic or anodic peak of about the same magnitude of the peak formed during the forward scan. As the scan rate was increased, the peak current shifted to more negative potentials which also indicates the irreversibility of the system.

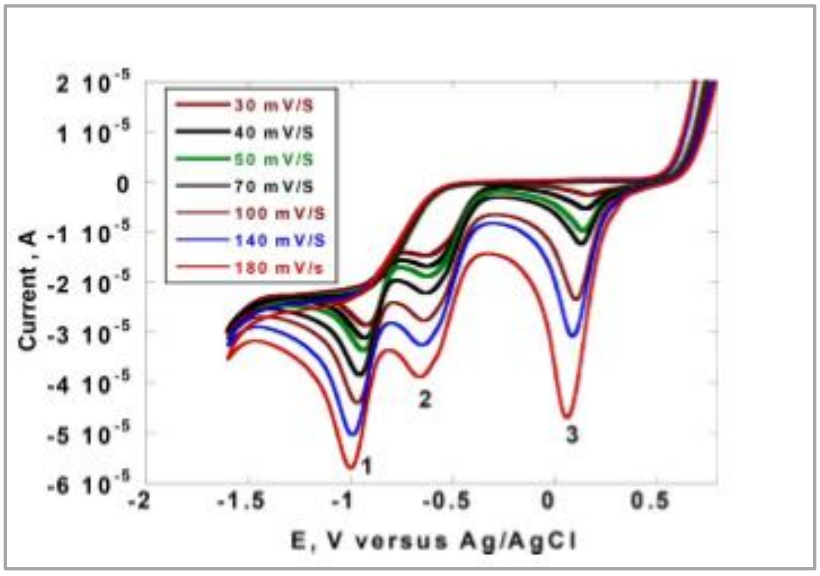

Figure 13. Scan rate dependence of albendazole. (1.8 x 10^{-3} M) ABZ dissolved in acetonitrile containing 0.05 M TBAB at scan rates taken from 30-180 mV/s.

The resulting peak current for the three peak waves was found to increase linearly as the scan rate was increased. This linear relationship can be observed in Figure 14 obtained by plotting the peak current versus the scan rate from 30 mVs^{-1} to 180 mVs^{-1} for the three peaks. However, at higher scan rates (10-1000 mV/s), the peak current is no longer linear with increasing scan rate but preserves its linear relationship with the square root of the scan rate as it can be observed in figure 15 (peak centered at around -1.0 V).

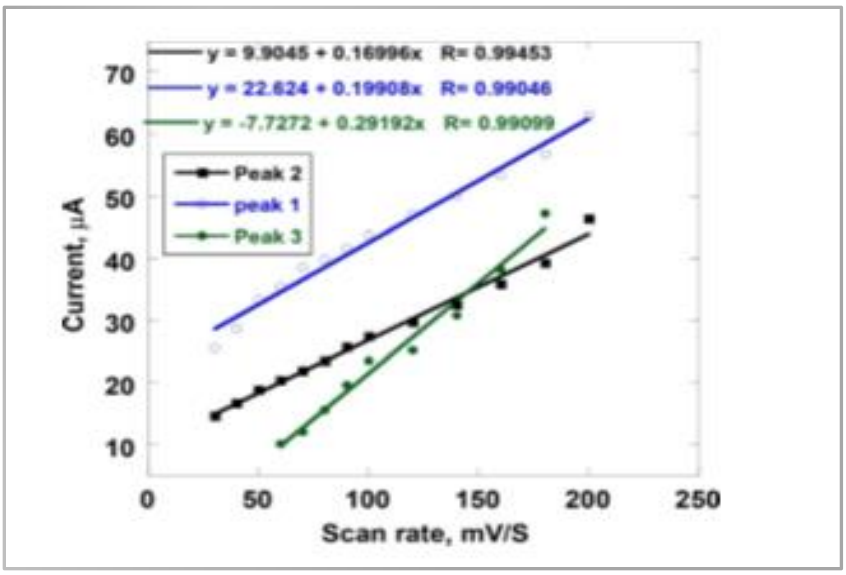

Figure 14. Peak current as a function of scan rate. (1.8 x 10^{-3} M) ABZ in acetonitrile containing 0.05 M TBAB for the three peaks in figure 17.

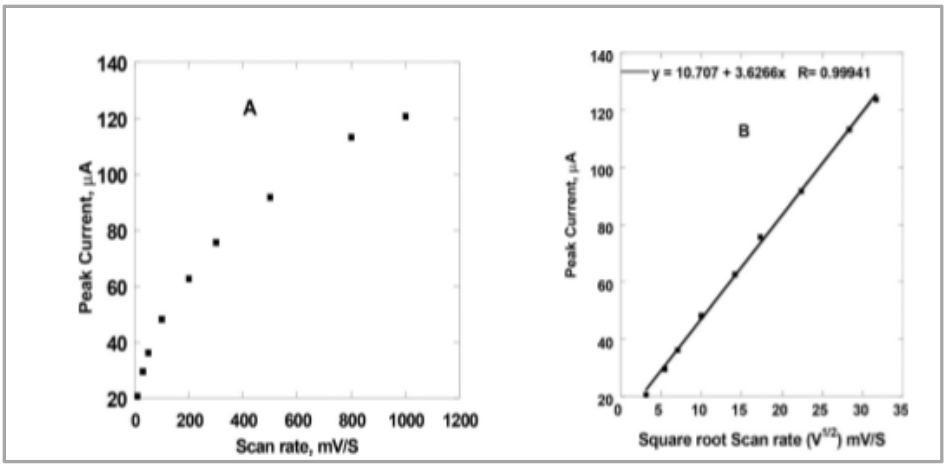

Figure 15. Peak current of ABZ at scan rates of 10-1000 mV/s. (1.8 x 10^{-3} M) ABZ in acetonitrile containing 0.05 M TBAB for the third peak centered around -1.0 V versus Ag/AgCl: A) peak current versus scan rate B) peak current versus square root of scan rate.

A linear relationship between peak current and square root of scan rate ($V^{1/2}$) suggests a diffusion-controlled reduction process on the electrode surface as it is generally accepted [68-69]. During cyclic voltammetry studies, the current produced due to an electrochemical reaction can be visually observed by studying the obtained cyclic voltammogram. The peak current represents the current that diffuses to the electrode surface during the electrochemical reaction and can be described by equation 4 below.

$$i_p = 0.229 \times 10^5 n(\alpha n_\alpha)^{1/2} AC^* D^{1/2} V^{1/2} \qquad \text{Equation 4}$$

Where *A* is the electrochemically active surface area, *D* is the diffusion coefficient, *C** is the bulk concentration of the analyte, n represents the number of electrons transferred during the reaction, α is the coefficient of electron transfer, and $V^{1/2}$ is the square root of the scan rate. The average diffusion coefficient for the electro-reduction of ABZ was estimated to be 0.143 x 10^{-8} cm^2/s using the slope of the lines of Figure 16 and equation 4.

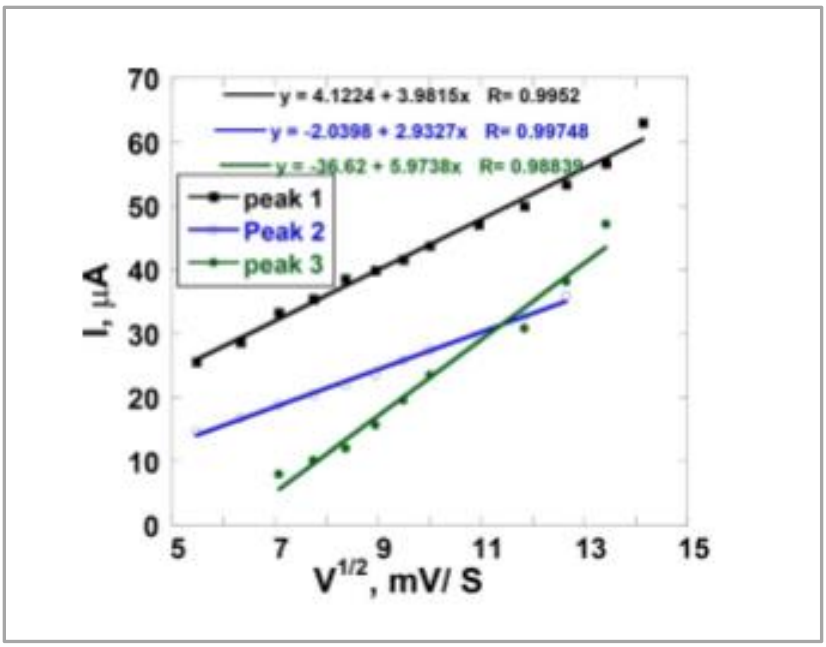

Figure 16. Peak current as a function of square root of scan rate. (1.8 x 10^{-3} M) ABZ in acetonitrile containing 0.05 M TBAB for the three peaks in figure 13.

The value of αn can be calculated from the slope of the line in Figure 17 (E_p vs. log *v*). For an irreversible electrode process, the linear relationship between peak potential and logarithm of the scan rate can be expressed by equation 5 [59, 70].

.

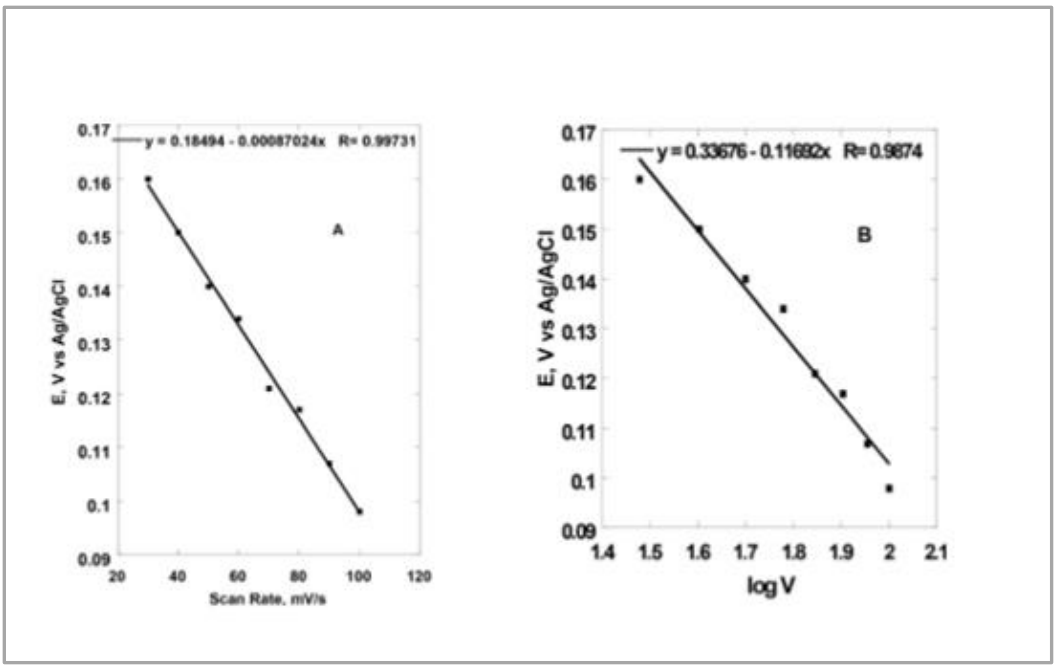

Figure 17. Peak potentials (E_P) of (1.8 x 10^{-3} M) ABZ in acetonitrile containing 0.05 M TBAB on gold electrode for the second peak wave. A represents the plot of E_P versus scan rate, and B represents E_P versus log scan rate.

$$E_p = E_0 + \left[\frac{2.303RT}{\alpha nF}\right]\log\left|\frac{RTK^\circ}{\alpha nF}\right| + \left|\frac{2.303RT}{\alpha nF}\right|\log v \qquad \text{Equation 5}$$

Where E_p represents the peak potential, E_0 is the formal potential, T is the temperature in Kelvin (298), R is the gas law constant (8.314), F (Faraday constant = 96480), k^o is the standard heterogeneous rate constant, α is the transfer coefficient, n is the number of electrons transferred, and *v* represents the scan rate. The slope was -0.117 and αn was found to be 0.513. For the third peak αn was calculated similarly and was found to be 0.496.

Bulk electrolysis analysis. The three reduction waveforms observed on the cyclic voltammograms (Figure 13), indicate that three different species were formed at the gold electrode surface during the CV analysis of ABZ. To investigate the species formed, bulk electrolysis was carried out to completely electrolyzed the solution and obtain quantifiable amounts of the products. The electrolysis was carried over a period of seven hours using a gold working electrode, and the potential was set at -1.5 V versus Ag/AgCl. 7.5×10^{-3} M ABZ solution was constantly stirred during electrolysis to maintain a continuous flow of fresh solution to the electrode surface. This type of mass transport technique is a simple way of transferring the analyte molecules to the electrode surface and achieve complete electrolysis. Complete electrolysis of the ABZ molecules is important to recover the necessary amount of product for further characterization. The reduction products were monitored every hour using HPLC-MS analysis.

HPLC-MS analysis of reduction products. In order to characterize the reduction products of albendazole, 100 μL aliquots of the electrolyzed solution were drawn out every hour and diluted to 1mL before filtration using a 0.45 nm filter. Liquid chromatography analysis revealed three major peaks with retention times at 3.4, 3.9 and 4.4 minutes. The peak at 3.9 minutes corresponds to unreacted ABZ. The peaks at 3.4 and 4.4 minutes corresponds to the reduction products of ABZ. The chromatogram (Figure 18) shows a clear increase in the product eluding at 3.4 minutes (peak 1) as the time of the electrolysis increases. The product eluting at 4.4 minutes (peak 3) appeared after one hour of electrolysis, and its concentration seems to be higher than that of the product eluding at 3.4 minutes. Peak 3 increased consistently with the time of electrolysis from 1hour to 4 hours. However, after seven hours of electrolysis peak 3 decreased noticeably,

and peak 1 experienced higher increase. This could indicate that the product eluding at 3.9 minutes is reacting to form more of the product eluding at 3.4 minutes. The concentration of ABZ remained higher than any of the products formed at any time during the electrolysis indicating that only a small percentage of the drug was being reduced during the seven hours process.

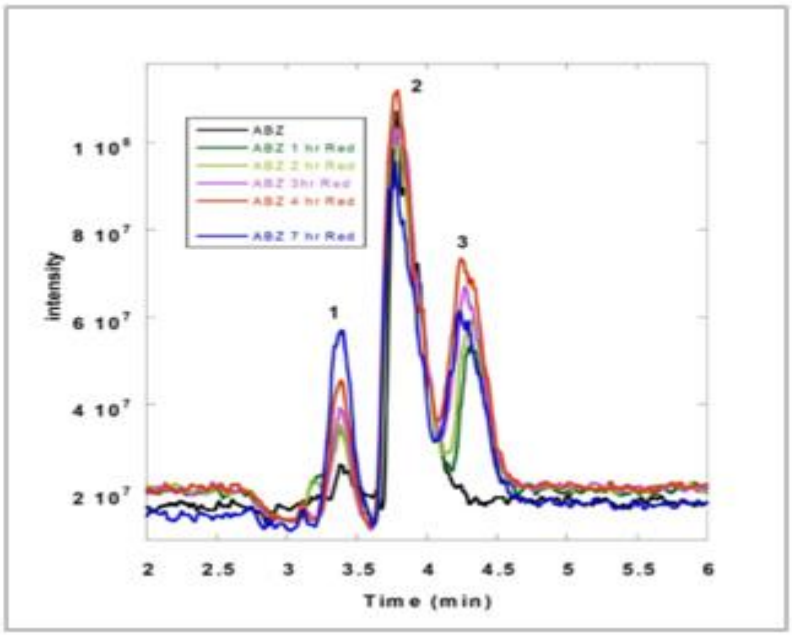

Figure 18. Chromatographic analysis of albendazole after electrolysis at – 1.5 V for seven hours.

The products formed during the bulk electrolysis of albendazole were further analyzed using mass spectrometry in an attempt to identify them. The pure ABZ eluted at 3.9 minutes (peak 2) on the HPLC chromatogram (Figure 18). The mass spectrum of peak 2 includes M/Z of 265, 234, and 307 (Figure 19). The mass spectra of the products eluted at 3.4 minutes (Figure 20) shows peaks with M/Z of 240 281, and 284. The

presence of peaks with higher M/Z than the initial molecule could indicate initial oxidation of albendazole to ASOX. However, further analysis is needed in order to identify the products formed during the electrochemical reduction of albendazole.

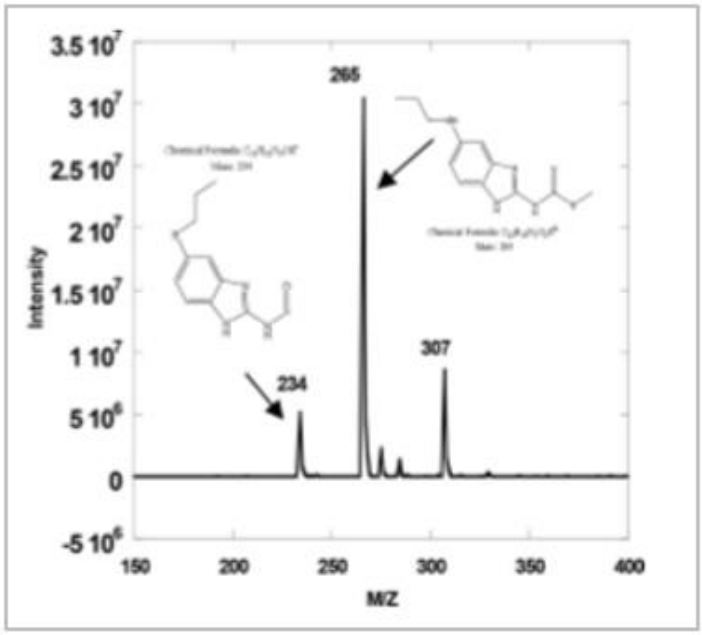

Figure 19. Mass spectrometry of albendazole after electrolysis at – 1.5 V for peak eluding at 3.9 minutes.

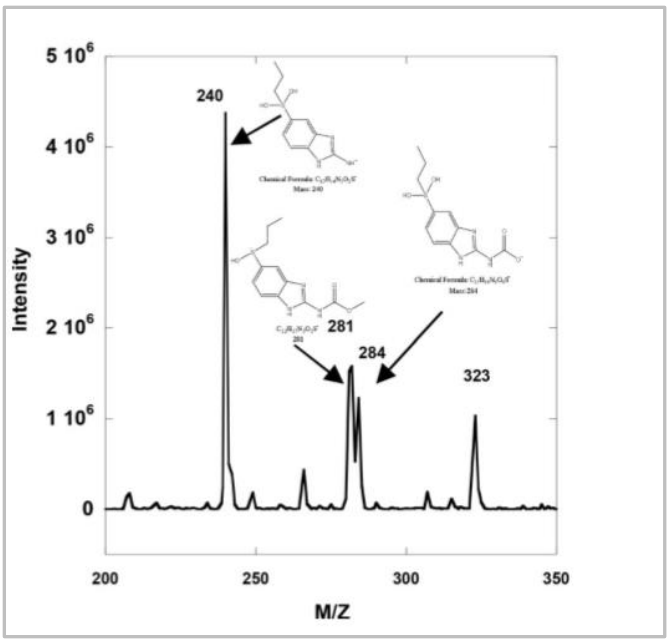

Figure 20. Mass spectrometry of albendazole after electrolysis at – 1.5 V for peak eluding at 4.35 minutes.

Conclusion

The cyclic voltammogram obtained during the electrochemical reduction of ABZ on gold electrode surface, suggests the formation of three reduction products. By examining the CV at different scan rates, it can be asserted that the electrode process was irreversible and limited by diffusion-controlled mass transport. The reactions on the electrode surface followed and ECE mechanism which allowed the formation of the products by an electron transfer reaction followed by a chemical step. αn was calculated to be 0.513 and 0.496 for the second and third peak respectively. The reduction products of ABZ could not be accurately identified using the obtained HPLC-MS results. Further work should include isolation of ABZ reduction products for characterization using techniques such as IR and NMR.

Chapter 4

Electrochemical Reduction of Artemisinin

Introduction

Artemisinin (Art) and its derivatives (i.e., dihydroartemisinin and artemether) constitute the front-line treatment for malaria worldwide. Art is isolated from the Chinese plant Artemisia Annua. The use of Artemisia Annua in traditional Chinese medicine dates to 168 B.C. for the treatment of fever, helminth infections, and malaria [71]. The isolation and structure elucidation of artemisinin was published in 1972 by the Chinese scientist Youyou Tu who was partially awarded the 2015 Nobel Prize for medicine for this discovery [72]. Artemisinin is an enantiomerically pure sesquiterpene lactone. Its pharmacophore consists of a 1, 2, 4 trioxane ring containing an endoperoxide bridge (Figure 21). Art is very effective against Plasmodium falciparum, the malaria-causing parasite. Unfortunately, studies have reported that plasmodium falciparum is becoming resistant to artemisinin. Currently, an artemisinin-based combination therapy (ACT) is being used to slow down the parasite resistance mechanism. Artemisinin is also being investigated as a potential anti-cancer agent. Studies have found that it is highly active against different cancer cell lines such as leukemia, colon, and breast cancer [73]. In this study, the electrochemical reduction behavior of artemisinin was investigated using cyclic voltammetry and bulk electrolysis. The reduction products were analyzed using HPLC, and HPLC-MS.

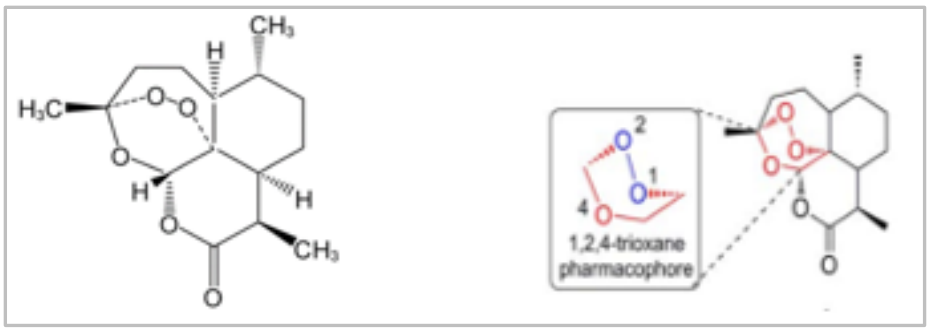

Figure 21. Structure of artemisinin, a sesquiterpene lactone-containing a 1, 2, 4-trioxane ring pharmacophore.

Experimental Methods

Chemicals. Artemisinin was purchased from Tokyo Chemical Industry Co., TLD. Tetrabutylammonium bromide (TBAB) was purchased from WWR (West Chester, PA). The artemisinin solutions (0.03 M) were prepared using acetonitrile as the solvent and 0.05 M TBAB being the supporting electrolyte. A 50:20:30 mixture of Acetonitrile, methanol, and deionized water were used for the mobile phase.

Bulk electrolysis/cyclic voltammetry procedures. The electrochemical analysis was carried out with a computer controlled electrochemical workstation (CHI 660c, USA) with 98% ohmic drop (IR) compensation. A bulk electrolysis electrochemical cell was used for all electrochemical experiments. A gold electrode was used as working electrode for cyclic voltammetry analysis. Before use, the gold electrode was polished using 1 µm diamond polishing paste then ultra-sonicated in ethanol and distilled water successively for 1 min followed by rinsing with water. The electrolysis of artemisinin was carried out in ammonium bromide-acetonitrile solution under stirring conditions for 3hours. The potential of the reaction was fixed at 1.5 V versus Ag/ AgCl. 0.5 mL aliquots of the reaction mixture were withdrawn every hour then filtered and analyzed using

chromatographic and mass spectrometry techniques. The solvents used were compatible with the mobile phase.

HPLC procedure. The HPLC analysis of artemisinin reduction products was carried out on a ZORBAX C-18 300SB column (4.6 x150 mm long and with 3.5 µm particle size, Agilent Technologies). The mobile phase consisted of acetonitrile, methanol and de-ionized water (50:25:25) respectively with 0.1% formic acid. The HPLC-UV analysis was carried out using Agilent 1100 series HPLC unit equipped with an UV-Visible detector with the wavelength set at 254 nm. The chromatographic run was performed under isocratic conditions at the flow rate of 100 µL /min.

Mass spectrometry procedure. The mass spectrometer (LC/MS Ion Trap 1100 series) was set to ESI in positive ion mode. Additional settings of the mass spectrometer were as follows: Scan mode (standard), range (50-2200) m/z, speed (13,000 m/z/min), threshold (1000), nebulizer gas (15.0 psi), and dry gas (5.0 L/min), dry temp (325 °C). The target mass was set to 282 while the compound stability and trap drive level were set to 100%. The ramp range was from 4500.0 to 1500.0 V. The ms/ms fragmentation amp was set to 1.00 V.

Results and Discussion

Bulk electrolysis/cyclic voltammetry analysis. Bulk electrolysis and cyclic voltammetry analysis of artemisinin were performed using the same setup and conditions except the working electrodes were different. The objective of bulk electrolysis was to reduce a 0.03M solution of artemisinin in quantitative amounts with the purpose to characterize and identify the reduction products. Aliquots of the reaction mixture were withdrawn every hour then filtered and analyzed using chromatographic and mass

spectrometry techniques. Cyclic voltammograms for the artemisinin solution were recorded at 30 minutes intervals during electrolysis. The cyclic voltammograms at 0, 30, and 60 minutes are shown in Figure 22.

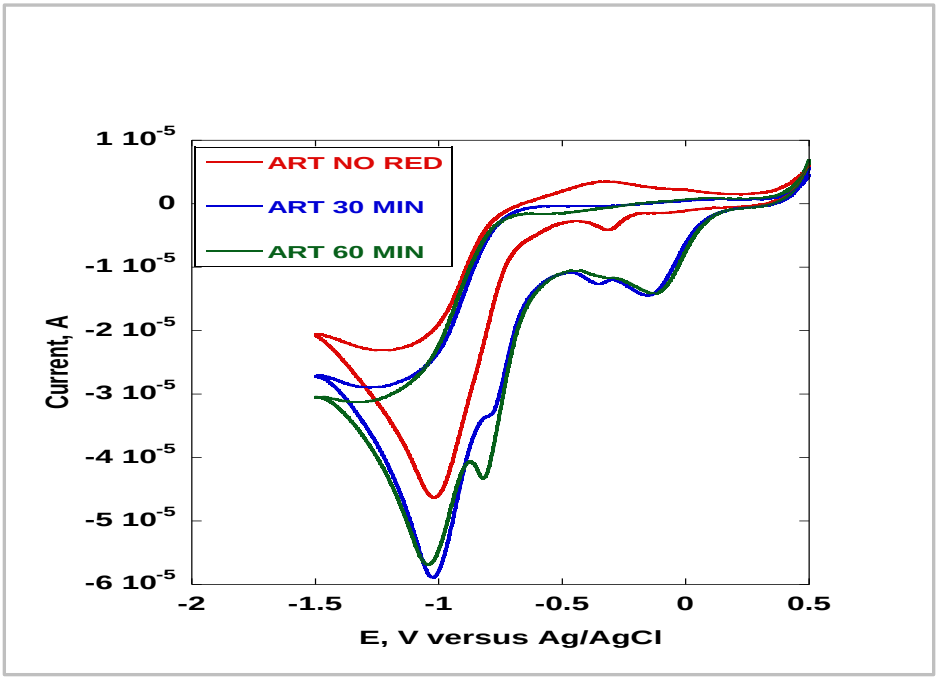

Figure 22. Cyclic voltammograms of Art and electrolyzed Art solutions. The CVs were taken after 30 min and 60 min of electrolysis using a gold working electrode at 1.5 V potential.

The voltammograms taken at 30, and 60 minutes show electrochemical reduction of Art as compared to the voltammogram of Art before electrolysis. The broadening of existing peaks and formation of new peaks is evidence of reduction product formation. Mugweru et al. [74] performed a detailed study of the electron transfer characteristics of artemisinin on three different types electrode, a gold (Au), glassy carbon (GC), and

pyrolytic graphite (PG) working electrodes. The gold electrode was determined to have greater sensitivity towards the reduction of Art. Therefore, the kinetic parameters for the electrochemical reaction were obtained using a gold working electrode. According to Mugweru et al. [74], the reduction of Art on gold electrode surface is diffusion controlled and follows an EC mechanism. The kinetic parameters obtained on this study are reported here (Table 2).

Table 2

Electrochemical parameters for reduction of artemisinin on gold (Au), glassy carbon (GC), and pyrolytic graphite (PG) working electrodes.

Type of working electrode	Average current density (μAcm^{-2}) at $100mVs^{-1}$	Diffusion coefficient (D) (cms^{-1})	Electron transfer coefficient (αn)	Number of electrons transferred (n)	Rate constant (k_h)
Gold (Au)	4.62	3.34×10^{-6}	0.496	$1.52 \approx 2$	23 $cm\ s^{-1}$
GC, PG	1.28, 1.53	--	--	--	--

HPLC-MS analysis. The chromatograms in Figure 23 suggest reduction of Art and product formation as a function of electrolysis time. The retention time of the drug before reduction was determined to be at 25.8 minutes (Figure 23a). After one hour to three hours of electrolysis, the development of new peaks due to the formation of reduction products is clear as figures 23b and 23c show. To identify the products formed by the electrolysis of artemisinin, the solutions were analyzed by mass spectrometry. Figure 24a shows the mass spectrum of Art before reduction. The molecular ion can be identified with a mass of 282.8, m+1 (283.8), m+2 (284.8) and m + sodium (m+23)

(304.8). The mass spectra of electrolyzed Art solutions show masses of possible reduction products. Reduction of Art at the C=O bond produces dihydroartemisinin and the loss of oxygen from the peroxide bridge produces deoxy artemisinin (Figure 24b). According to the mass spectra, it can be deduced that these two products were formed although further analysis is needed to confirm this result.

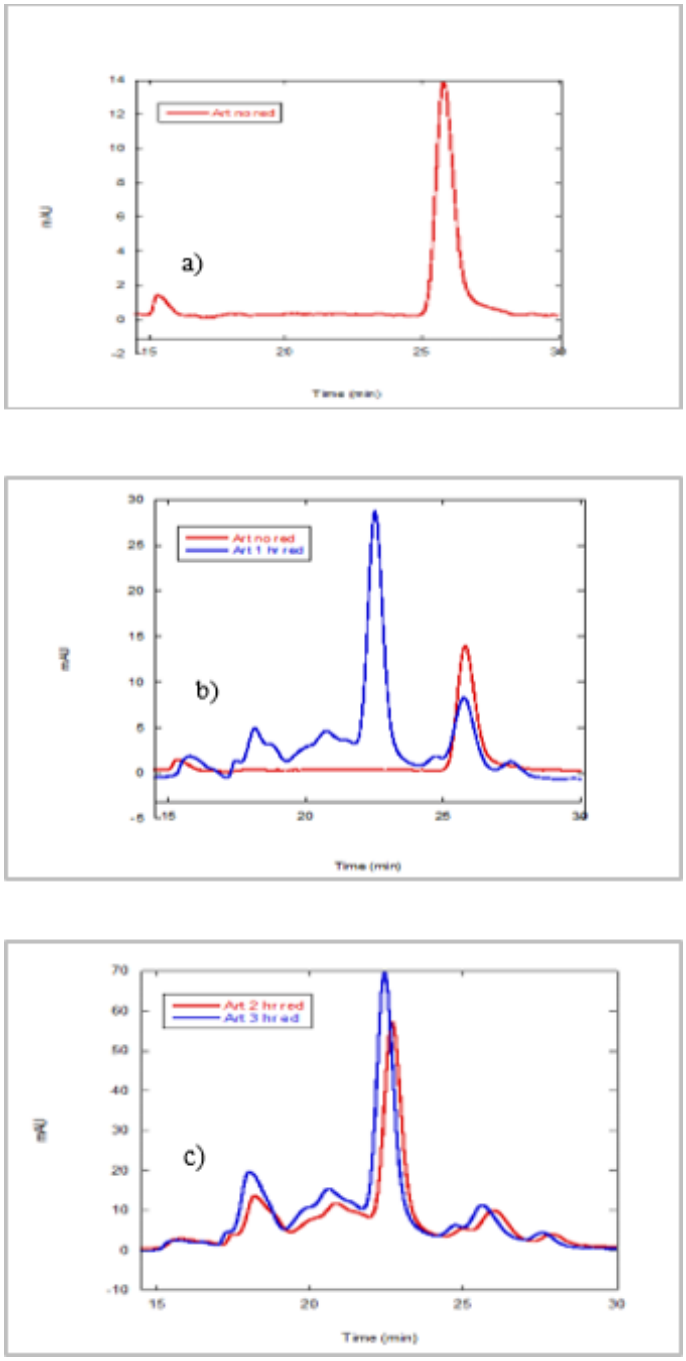

Figure 23. Chromatograms of artemisinin: a) before electrolysis; b) before and after 1 hr. of electrolysis; c) after 2 and 3 hours of electrolysis.

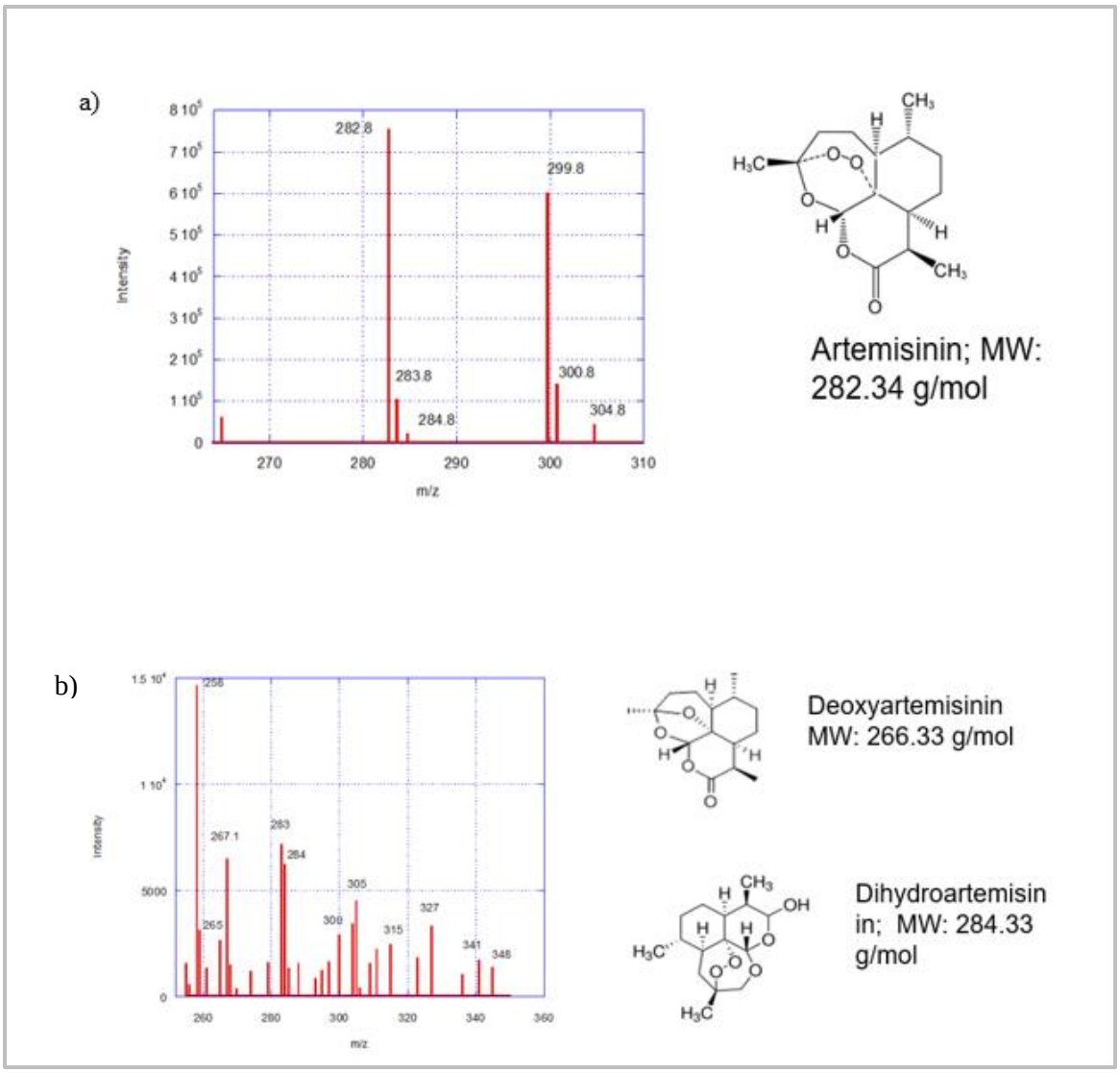

Figure 24. Mass spectrometry of artemisinin: a) before electrolysis showing m/z corresponding to artemisinin and; b) after 3 hrs. of electrolysis showing m/z for possible reduction products deoxy artemisinin and dihydroartemisinin.

Conclusion

Electrochemical reduction of artemisinin was performed during this work. Bulk electrolysis of Art, for a three hours period at a fixed reductive potential (1.5 V versus Ag/ AgCl), yielded reduction products as the HPLC analysis showed. The cyclic voltammograms taken at 30 minutes intervals during electrolysis corroborate these findings. Dihydroartemisinin and deoxy artemisinin are thought to be among the products formed. Reduction of Art on gold electrode surface follows and EC mechanism. The electron process is irreversible and limited by diffusion controlled mass transport as reported by [74].

Chapter 5

Hemoglobin Catalyzed Bioactivation of Artemisinin

Introduction

The action of artemisinin against malaria parasites is thought to be heme-mediated, although as of now the detailed mechanism has not been reported [75]. Understanding the precise mode of action of artemisinin will allow the design of more potent analogs for malaria and cancer treatments, and aid in deciphering the resistance mechanism from the malaria parasite. plasmodium falciparum goes through several stages of development within the host's red blood cells. Throughout its development, the parasite ingests and degrades most of the hemoglobin in host's cells. Due to this process, the parasite digestive vacuole is rich in iron provided by the heme prosthetic group of hemoglobin [76]. Artemisinin is highly selective towards plasmodium falciparum-infected red blood cells. This observation can be used to rationalize the iron-dependent bio-activation of the endoperoxide group of artemisinin [75]. Currently, there are two proposed pathways for artemisinin bio-activation the reductive cleavage model and the open peroxide model. The reductive cleavage model proposes that artemisinin bio-activation is triggered by the reduction of the endoperoxide bond by Fe (II) to generate oxygen radicals. The highly reactive oxygen radicals rearrange to generate carbon-centered radicals. Primary and secondary carbon-centered radicals have been detected after iron activation using electro-paramagnetic resonance spin-trapping techniques. Proponents of the open peroxide model argue that carbon radicals cannot exist long enough to have any intramolecular interactions. Instead, they propose that artemisinin acts as a source of hydrogen peroxide which undergoes a Fenton like reaction to produced hydroxyl radicals

capable of irreversibly damaging proteins and other macromolecules. In this model, iron behaves like a Lewis acid and facilitates the cleavage of the endoperoxide bond. The non-peroxidic oxygen is believed to provide stabilization to lower the amount of energy required to break the oxygen bridge [75].

The principal molecular target of artemisinin is yet to be identified. The fact that artemisinin can produce different reactive intermediates including carbon and hydroxyl radicals indicates that it can interact with a wide range of macromolecules. Various research groups have reported the identification of heme-artemisinin adducts by mass spectrometry [76]. These findings suggest that inhibition of globin formation and accumulation of heme within the malaria parasite and cancer cells can cause parasite death and cancer cells apoptosis. Other proposed molecular targets of plasmodium falciparum are proteins, cell membranes, and mitochondria. Oxidative stress has been reported as a cause of cancer cell apoptosis. The mechanism of action of artemisinin within cancer cells is believed to be similar the mechanism that causes death to malaria parasites. On the other hand, some studies have identified DNA damage caused by artemisinin that is independent of oxidative stress. In this research, the reductive mode of artemisinin bio-activation was investigated using a carbon nanofibers/hemoglobin-based electrochemical biosensor.

Experimental Methods

Chemicals. Artemisinin was purchased from Tokyo Chemical Industry CO. LTD. Acetonitrile, methanol was purchased from VWR. **PSS**, Carbon nanofibers and hemoglobin (Hb, MW 66,000) were purchased from Sigma Chemical Co. The nanofibers had a diameter 100 nm diameter and a variable length between 20-200 μm. They were

used without further purification. A concentrated (0.004 M) ART solution was made in 20 mM acetate buffer pH 5.5 containing 1% methanol. The solution was used as a stock solution for all other experiments. Hemoglobin was used without any additional purification. All other chemicals were HPLC grade.

Electrochemical procedures. Cyclic voltammetry and amperometric analysis were carried out with a computer controlled electrochemical workstation (CHI 660c, USA) with 98% ohmic drop (IR) compensation. A three-electrode electrochemical cell was used for all electrochemical experiments. A glassy carbon electrode (0.07 cm^2) and a pyrolytic carbon electrode were used as working electrode while a platinum wire as counter electrode. The Ag/AgCl reference electrode was equipped with a glass tip separated from the sample solution compartment by a salt-bridge containing saturated KCl and terminating in a medium porosity glass frit. Before use, glassy carbon electrodes were polished using 1 µm diamond polishing paste then ultra-sonicated in ethanol and distilled water successively for 1 min followed by rinsing with water. All electrochemical measurements were carried out under ambient conditions.

Hemoglobin/PSS biosensor preparation. A pyrolytic Carbon working electrode was used to prepare the biosensor. A thin slice of the electrode was cut off to expose a pristine electrode surface before the assembly. 2µL of a 45mg/ml of hemoglobin solution in acetate buffer (pH 5.5) was set on the pyrolytic carbon electrode surface and then left to dry at room temperature. A second layer consisting of 2µL of PSS solution in DI water was set on the hemoglobin modified electrode and allowed to dry at room temperature. The electrode was rinsed with DI water to removes any unattached material. The electrochemical cell contained 10 ml of 20 mM acetate buffer pH 5.5 as the supporting

electrolyte solution. To avoid oxygen interference, the electrolyte solution was purged with nitrogen gas (N_2) for five minutes to remove the oxygen before the analysis.

Hemoglobin/CNFs biosensor preparation. The biosensor was assembled using a glassy carbon (GC) electrode. The GC electrode surface was modified using carbon nanofibers (CNFs). 2 µL of a 2mg/ml suspension of CNFs in DMS was carefully placed on the surface of a previously cleaned GC electrode and allowed to dry at room temperature. A second layer consisting of 2µL of a 45mg/ml of hemoglobin solution in acetate buffer (pH 5.5) was set on the CNFs modified electrode and allowed to dry at room temperature. The electrochemical cell contained 10 ml of 20 mM acetate buffer pH 5.5 as the supporting electrolyte solution. To avoid oxygen interference, the electrolyte solution was purged with nitrogen gas (N_2) for five minutes to remove the oxygen prior to the analysis.

Results and Discussion

Hemoglobin/polystyrene sulphonate (PSS) biosensor. Hemoglobin is an oxygen-transporting protein found in red blood cells. It includes four heme prosthetic groups each containing an iron molecule in the center. Due to the presence of Iron (II), the heme groups are electroactive which makes hemoglobin an ideal recognition molecule for assembling electrochemical biosensors. Immobilization of hemoglobin on the electrode surface is a critical step since the immobilization procedure may alter its normal behavior. Hemoglobin's conformation must be kept intact for it to remain active after immobilization. There are many different methods for immobilizing enzymes onto the electrode. One of the simplest methods is to entrap the enzyme between the electrode and a dialysis membrane or a polymeric film. This biosensor was prepared by entrapping

a hemoglobin solution between the surface of a pyrolytic carbon electrode and a film of polystyrene sulfonate. Several layers of hemoglobin and PSS were assembled to improve the results. The voltammogram taken before purging with nitrogen showed a well define reduction peak due to the presence of oxygen in solution. After purging the solution with nitrogen gas, the cyclic voltammetric results did not show well-defined reduction and oxidation peaks. Well-defined redox peaks are expected after purging. Otherwise, the biosensor may not be assembled correctly. These results could indicate that good contact between hemoglobin and the sensing material was not achieved or that the enzyme was denatured during the assembly. A different method using carbon nanofibers to immobilize hemoglobin was utilized to continue the experiment.

Carbon nanofibers (CNFs)/ hemoglobin biosensor. Carbon nanomaterials such as carbon nanotubes, graphite powder, and carbon nanofibers are ideal materials for construction of biosensors due to their excellent conductivity, large surface area, and biocompatibility. According to Vamvakaki et al. [77], carbon nanofibers are superior to carbon nanotubes or graphite powder for direct immobilization of enzymes onto their surface since CNFs have larger functionalized surface area. Also, CNFs' high porosity and absorption ability support enzyme immobilization [78]. Therefore, CNFs were preferred to assemble this biosensor. A layer consisting of 2 µL of a 2mg/ml suspension of CNFs in DMS was placed on the polished glassy carbon electrode's surface and allowed to dry. Subsequently, a layer of the hemoglobin solution was placed on the CNFs modified electrode and allowed to dry before analyzing it. Figure 2 shows a schematic of the biosensor assembly.

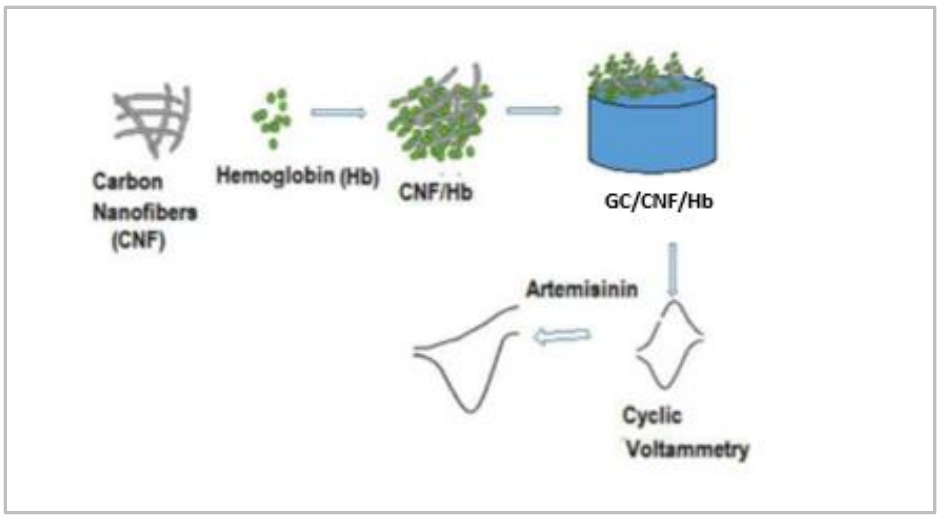

Figure 25. Schematic representation for assembly of GC/CNFs/Hb biosensor.

The biosensor was tested prior to the study of artemisinin by evaluating hemoglobin bioactivity using cyclic voltammetry. After purging the solution with nitrogen to drive out the oxygen, reduction and oxidation peaks are observed due to the redox reaction of iron in hemoglobin. During the forward scan iron (II) is oxidized to iron (III) while during the reverse scan iron (III) is reduced and becomes iron (II) again. Consistent results after purging the solution confirm the reliability of the biosensor and the favorable conformation and bioactivity of hemoglobin. Artemisinin was added to the electrochemical cell containing 10 ml of acetate buffer. 0.2 ml of artemisinin solution was added incrementally to obtain greater concentration after each addition. The solution was analyzed after each Art addition using cyclic voltammetry. Figure 26 shows the cyclic voltammogram of some selected concentrations of artemisinin. As clearly illustrated in the figure, the voltammogram at 0.0 μM of artemisinin is completely reversible. This is due to the iron in hemoglobin been oxidized and subsequently reduced at the electrode surface. After addition of 0.8 μM of artemisinin, the oxidation peak is

noticeably decreased, and the reduction peak increases. This trend continues as the concentration of artemisinin is increased. At 5.8 µM, the oxidation peak is mostly gone.

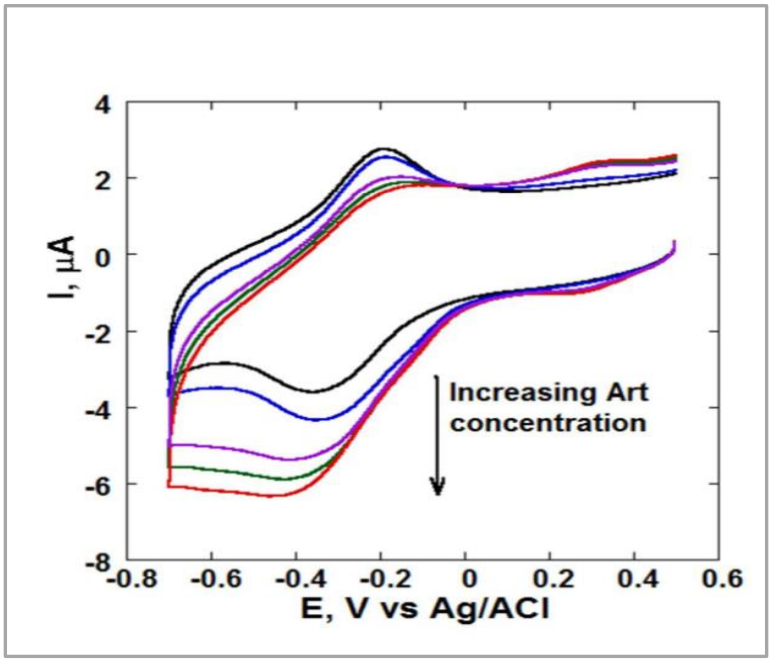

Figure 26. Cyclic voltammograms obtained from reduction of Art using Hb/CNFs biosensor, at (0.0 µM, 0.8 µM, 1.2 µM, 2.6 µM, 5.8 µM) of artemisinin.

In this case, artemisinin is being reduced by iron (II) which is consequently oxidized to iron (III). The results indicate that hemoglobin catalyzes artemisinin's peroxide bridge reduction and subsequent radical formation is possible. Studies have shown that after reduction of artemisinin, oxygen and carbon-centered radicals are formed [79]. These very reactive radical species are thought to be responsible for the eradication of the malaria parasite and cancer cells.

Hemoglobin-catalyzed reduction of artemisinin. Reduction of artemisinin on glassy carbon electrode surface was investigated by Mugweru et al. [74]. The peak potential was found to be - 0.85 V versus Ag/AgCl reference electrode. In this work, peak potential of hemoglobin anchored onto carbon nanofibers is about -0.30 V vs. Ag/AgCl. The reduction potential of artemisinin on CNFs/Hb modified glassy carbon electrode averages at about – 0.375 V vs. Ag/AgCl. The results show the electrocatalytic effect of hemoglobin towards the reduction of artemisinin. The reduction potential of artemisinin was catalytically reduced by about 475 mV. Hemoglobin anchored on CNFs must be properly oriented such that the heme prosthetic group can interact with artemisinin during the electrochemical analysis. The catalytic activity of hemoglobin toward artemisinin correlates closely with the orientation of the heme groups in Hb [78]. A line Weaver-Burke plot (Figure 27) was obtained using the peak current produced with increasing concentration of artemisinin. The Michaelis–Menten constant (K_m) for Art reduction on CNF/Hb modified glassy carbon electrode was determined using the Weaver-Burke plot and equations 6 and 7.

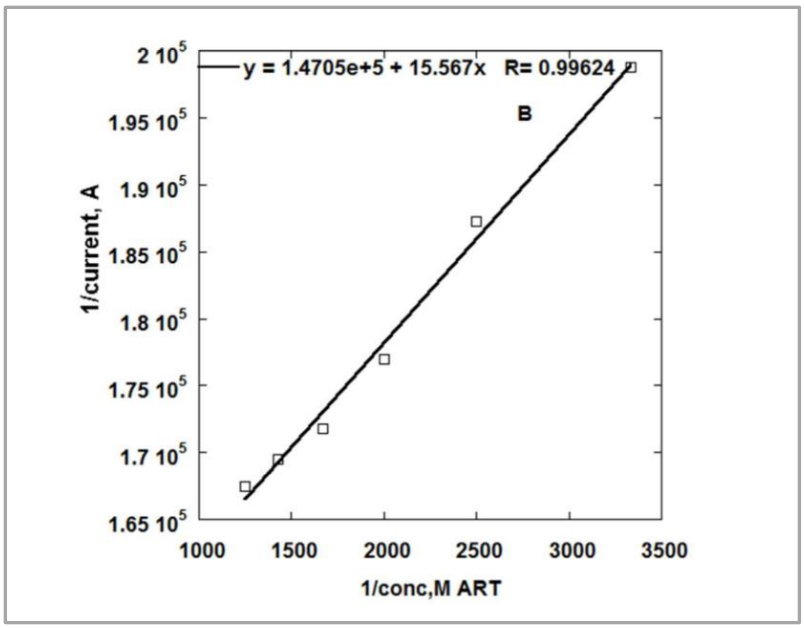

Figure 27. Line Weaver-Burk plot using GC/CNFs/Hb voltammograms.

$$I_{ss} = \frac{I_{\max}[Art]}{k_m + [Art]} \qquad \text{Equation 6}$$

$$\frac{1}{I_{ss}} = \frac{1}{I_{\max}} + \left[\frac{k_m}{I_{\max}}\right]\frac{1}{Art} \qquad \text{Equation 7}$$

Where K_m represents the Michaelis-Menten constant, which indicates the enzyme-substrate kinetics. I_{ss} is the steady-state current obtained from GC /CNF/Hb CV measurements. I_{max} is the maximum current obtained from CVs at saturated Art solutions. The apparent K_m for this system was found to be 0.093 mM according to the kinetic studies. Table 3 compares the K_m for hemoglobin from several literature articles and this

study based on the surface the enzyme is immobilized as well as the substrate under study. The K_m value for hemoglobin in solution is about three times smaller than that found in this study which makes sense given that the enzyme was not immobilized. Therefore, it was free to interact with the substrate.

Table 3

Michaelis-Menten constant (K_m) of hemoglobin immobilized on different materials' surfaces.

Materials	Substrates	K_m (mM)	References
Iron nanoparticles	Hydrogen peroxide	0.29	[80]
mesoporous silica	Hydrogen peroxide	2.87	[81]
in solution	Artemisinin	0.028	[82]
Carbon nanofibers	Artemisinin	0.093	This study

Effect of artemisinin concentration. Figure 26 shows cyclic voltammograms of GC/CNF/Hb modified electrode obtained at increasing concentration of Art. The peak current increases as the concentration of Art is increased. The catalytic peak current increases linearly with Art concentrations between 0 and 200 μM (Figure 28). This linear relationship was used to estimate the sensitivity of GC/CNF/Hb modified electrode for Art catalysis. The linear relationship showed the slope as 0.329 mA/mM with a regression coefficient of (R = 0.99436).

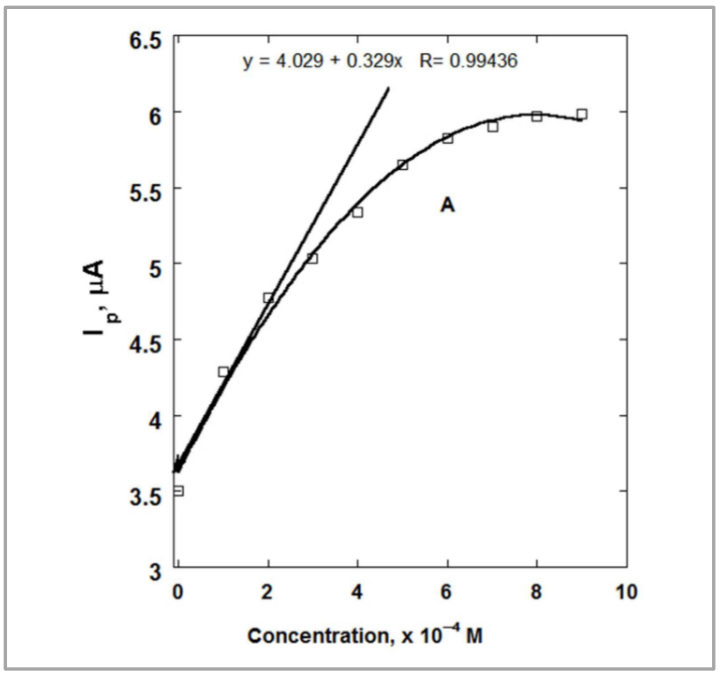

Figure 28. Current versus concentration of artemisinin obtained from cyclic voltammograms.

Effect of scan rate. The cyclic voltammogram of CNFs/Hb modified glassy carbon electrode at 100 mV/s exhibits well-defined redox peaks at −0.22 V and −0.38 V vs. Ag/AgCl (Figure 29). The formal potential ($E^{0'}$) was −0.30 V vs. Ag/AgCl. CVs were also taken at scan rates of 100 mV/s and 200 mV/s in the presence of 0.20 mM ART solution (Figure 30). At 200 mV/s, the CV exhibits both the oxidation and reduction peaks as in CVs taken in the absence of artemisinin while at 100 mV/s, the oxidation peak is gone. This indicates that at scan rates 100 mV/s and lower Art reacts with HbFe(II) rendering the system irreversible. The magnitude of the scan rate affects the system in that at higher scan rates, electron transfer between iron and the electrode is fast enough so that the chemical step does not occur. Therefore, a reversible behavior is observed.

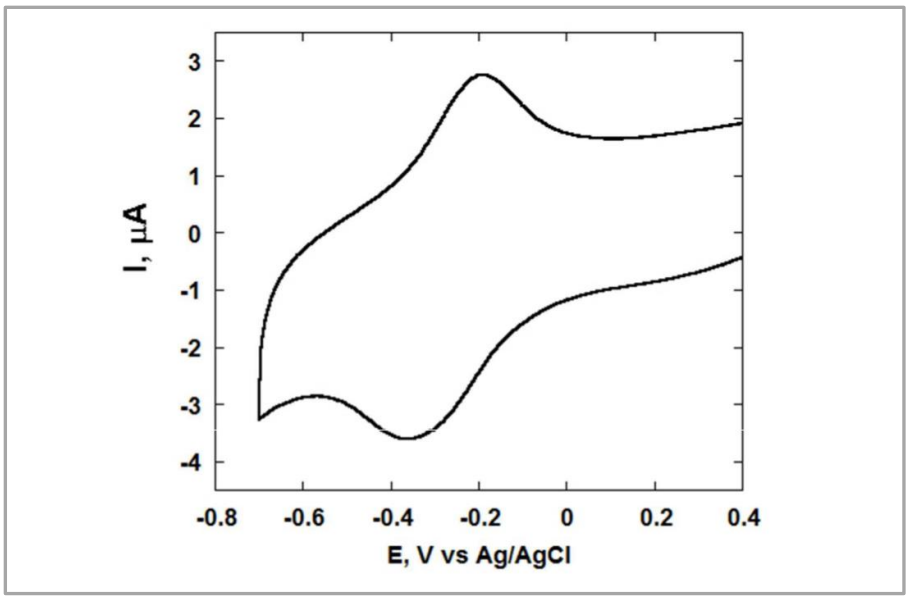

Figure 29. Cyclic voltammogram of CNFs/Hb modified GC electrode. CV taken in 20 mM acetate buffer pH 5.5 at 100 mV/s^{-1}.

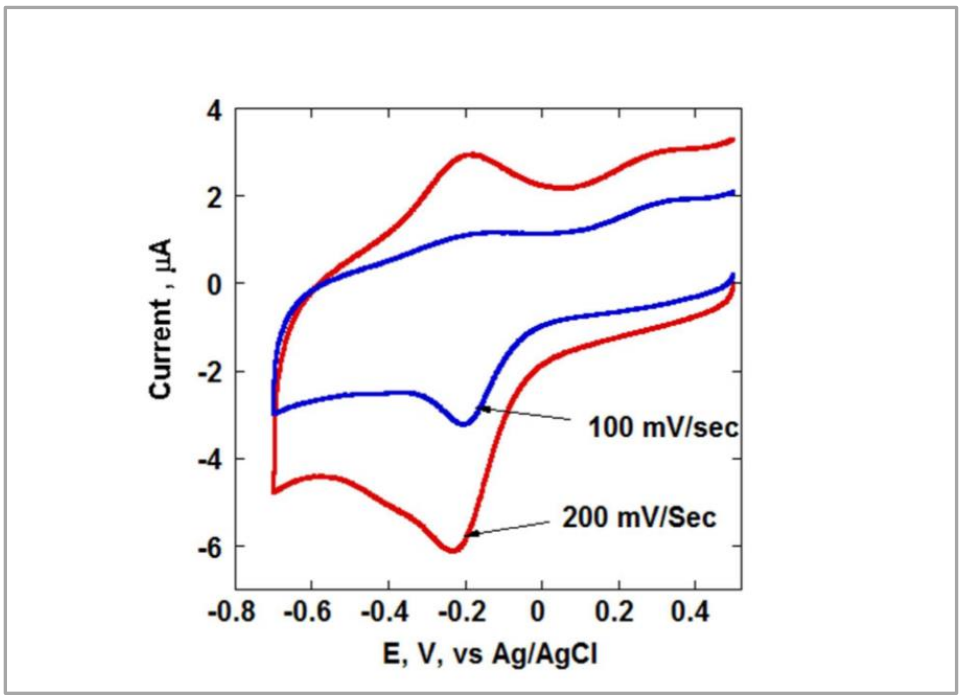

Figure 30. Cyclic voltammograms of GC/CNFs/Hb taken at 100 and 200 mV/s^{-1} scan rates. The CVs were carried out in 20 mM acetate buffer pH 5.5 containing 0.2 mM Art.

Amperometric analysis of CNFs/Hb biosensor. The CNFs/hemoglobin biosensor was analyzed further using Amperometry to confirm its reliability and corroborate the results obtained by cyclic voltammetry. For this experiment, the electrochemical cell was set up similar to that for cyclic voltammetry. Addition of constant amounts of artemisinin to the electrochemical cell, containing 10 ml of the electrolyte solution, was done at 200 seconds intervals to allow the resulting current to equilibrate. The resulting current due to the reduction of artemisinin increased as the concentration of artemisinin in solution was increased. These results suggest that the biosensor worked as expected and that reductive bioactivation of artemisinin by HbFe(II) occurred on the electrode surface.

Conclusion

A sensitive carbon nanofiber/hemoglobin biosensor was assembled which was able to detect catalytic bioactivation of artemisinin by heme-bound iron (Fe II) using cyclic voltammetry. The GC/CNF/Hb system was also able to detect increased Art concentration in solution. The catalytic current generated upon subsequent additions of 0.2 ml Art solution was proportional to the concentration of Art in the electrochemical cell. This result shows that the assembled GC/CNF/Hb biosensor can be used for the determination of unknown concentration of analytes. From the cyclic voltammograms obtained, it can be inferred that hemoglobin was strongly anchored onto the CNFs' surface. Well defined cathodic and anodic peaks were observed for the GC/CNF/Hb system in the absence of artemisinin. In the presence of artemisinin, a well-defined cathodic peak is observed. This implies that the conformation of hemoglobin in this system was very favorable. The Michaelis-Menten constant (K_m) of hemoglobin towards

Art reduction was 0.093 mM. From literature, other similar systems with hemoglobin immobilized on different materials generated higher K_m values.

References

1. Bard, A. J., Zoski, Cynthia G, Voltammetry Retrospective. *Analytical Chemistry* **2000**, 346-352A.

2. Flato, J. B., Renaissance in polarographic and voltammetric analysis. *Analytical Chemistry* **1972,** *44* (11), 75A-87a.

3. Ashley, K., Electroanalytical applications in occupational and environmental health. *Electroanalysis* **1994,** *6* (10), 805-20.

4. Farghaly, O. A.; Abdel Hameed, R. S.; Abu-Nawwas, A.-A. H., Analytical application using modern electrochemical techniques. *Int. J. Electrochem. Sci.* **2014,** *9* (6), 3287-3318, 32 pp.

5. Qin Xu, A.-j. Y., Rui Zhang, Xiaojun Bian, Da Chen, Xiaoya Hu, Application of Electrochemical Methods for pharmaceutical and Drug Analysis. *Current Pharmaceutical Analysis* **2009,** *5* (2), 144-155.

6. Chatten, L. G., Recent applications of electrochemical techniques to the analysis of pharmaceuticals. *J Pharm Biomed Anal* **1983,** *1* (4), 491-5.

7. De Abreu, F. C.; Ferraz, P. A. D. L.; Goulart, M. O. F., Some applications of electrochemistry in biomedical chemistry. Emphasis on the correlation of electrochemical and bioactive properties. *J. Braz. Chem. Soc.* **2002,** *13* (1), 19-35.

8. Scholz, F., Voltammetric Techniques of Analysis: The Essentials. *ChemTexts* **2015,** *1* (4).

9. Basáez, L.; Vanýsek, P., Transport studies of β-lactam antibiotics and their degradation products across electrified water/oil interface. *Journal of Pharmaceutical and Biomedical Analysis* **1999,** *19* (1), 183-192.

10. Bath, B. D.; Michael, D. J.; Trafton, B. J.; Joseph, J. D.; Runnels, P. L.; Wightman, R. M., Subsecond adsorption and desorption of dopamine at carbon-fiber microelectrodes. *Anal. Chem.* **2000,** *72* (24), 5994-6002.

11. Chu, X.; Shen, G.-L.; Jiang, J.-H.; Kang, T.-F.; Xiong, B.; Yu, R.-Q., Voltammetric studies of the interaction of daunomycin anticancer drug with DNA and analytical applications. *Analytica Chimica Acta* **1998,** *373* (1), 29-38.

12. Radi, A., Accumulation and trace measurement of chloroquine drug at DNA-modified carbon paste electrode. *Talanta* **2005,** *65* (1), 271-275.

13. Silva, M. L. S.; Garcia, M. B. Q.; Lima, J. L. F. C.; Barrado, E., Modified tubular electrode in a multi-commutated flow system: Determination of acetaminophen in blood serum and pharmaceutical formulations. *Analytica Chimica Acta* **2006,** *573-574* (Supplement C), 383-390.

14. Earles, C.; Schenk, J. O., Rotating Disk Electrode Voltammetric Measurements of Dopamine Transporter Activity: An Analytical Evaluation. *Analytical Biochemistry* **1998,** *264* (2), 191-198.

15. El-Maali, N. A., Voltammetric analysis of ceftazidime after preconcentration at various mercury and carbon electrodes: application to sub-ppb level determination in urine samples. *Talanta* **2000,** *51* (5), 957-968.

16. Fdez. de Betoño, S.; Arranz Garcia, A.; Francisco Arranz Valentín, J., UV-Spectrophotometry and square wave voltammetry at nafion-modified carbon-paste electrode for the determination of doxazosin in urine and formulations. *Journal of Pharmaceutical and Biomedical Analysis* **1999,** *20* (4), 621-630.

17. Goyal, R. N.; Gupta, V. K.; Bachheti, N., Fullerene-C60-modified electrode as a sensitive voltammetric sensor for detection of nandrolone—An anabolic steroid used in doping. *Analytica Chimica Acta* **2007,** *597* (1), 82-89.

18. Hammam, E., Determination of nitrofurantoin drug in pharmaceutical formulation and biological fluids by square-wave cathodic adsorptive stripping voltammetry. *Journal of Pharmaceutical and Biomedical Analysis* **2002,** *30* (3), 651-659.

19. Kotkar, R. M.; Desai, P. B.; Srivastava, A. K., Behavior of riboflavin on plain carbon paste and aza macrocycles based chemically modified electrodes. *Sensors and Actuators B: Chemical* **2007,** *124* (1), 90-98.

20. Hefnawy, M. M., Analysis of certain tranquilizers in biological fluids. *Journal of Pharmaceutical and Biomedical Analysis* **2002,** *27* (5), 661-678.

21. Solangi, A. R., Khuhawar, M.Y., and Bhanger, M.I., Adsorptive stripping voltammetric determination of fluoroquinolones in pharmaceuticals. *J. Food Drug Anal* **2005,** (13), 201–204.

22. Dogan, B. a. O., S.A, Electrochemical behavior of carvedilol and its adsorptive stripping determination in dosage forms and biological fluids. Electroanalysis. *Electroanalysis* **2005,** *17* (22), 2074–2083

23. Farghaly, O. A.; Taher, M. A.; Naggar, A. H.; El-Sayed, A. Y., Square wave anodic stripping voltammetric determination of metoclopramide in tablet and urine at carbon paste electrode. *Journal of Pharmaceutical and Biomedical Analysis* **2005,** *38* (1), 14-20.

24. Radi, A.; El-Sherif, Z., Determination of levofloxacin in human urine by adsorptive square-wave anodic stripping voltammetry on a glassy carbon electrode. *Talanta* **2002,** *58* (2), 319-324.

25. Zhuang, Q.; Chen, J.; Chen, J.; Lin, X., Electrocatalytical properties of bergenin on a multi-wall carbon nanotubes modified carbon paste electrode and its determination in tablets. *Sensors and Actuators B: Chemical* **2008,** *128* (2), 500-506.

26. Adhoum, N.; Monser, L., Determination of trimebutine in pharmaceuticals by differential pulse voltammetry at a glassy carbon electrode. *Journal of Pharmaceutical and Biomedical Analysis* **2005,** *38* (4), 619-623.

27. Debnath, C.; Haslinger, E.; Likussar, W.; Michelitsch, A., Determination of the antimalaria drug artemether in pharmaceutical preparations by differential pulse polarography. *Journal of Pharmaceutical and Biomedical Analysis* **2006,** *41* (2), 638-643.

28. Ibrahim, F.; El-Enany, N., Polarographic determination of ciclopirox olamine in pure substance and in different pharmaceutical preparations. *Il Farmaco* **2003,** *58* (12), 1313-1318.

29. Florou, A. B.; Prodromidis, M. I.; Karayannis, M. I.; Tzouwara-Karayanni, S. M., Flow electrochemical determination of ascorbic acid in real samples using a glassy carbon electrode modified with a cellulose acetate film bearing 2,6-dichlorophenolindophenol. *Analytica Chimica Acta* **2000,** *409* (1), 113-121.

30. Majidi, M. R.; Jouyban, A.; Asadpour-Zeynali, K., Voltammetric behavior and determination of isoniazid in pharmaceuticals by using overoxidized polypyrrole glassy carbon modified electrode. *Journal of Electroanalytical Chemistry* **2006,** *589* (1), 32-37.

31. Quintino, M. S. M.; Araki, K.; Toma, H. E.; Angnes, L., Amperometric quantification of sodium metabisulfite in pharmaceutical formulations utilizing tetraruthenated porphyrin film modified electrodes and batch injection analysis. *Talanta* **2006,** *68* (4), 1281-1286.

32. Tamer, A., Adsorptive stripping voltammetric determination of ofloxacin. *Analytica Chimica Acta* **1990,** *231* (Supplement C), 129-131.

33. Gupta, V. K.; Jain, R.; Radhapyari, K.; Jadon, N.; Agarwal, S., Voltammetric techniques for the assay of pharmaceuticals—A review. *Analytical Biochemistry* **2011,** *408* (2), 179-196.

34. Mabbott, G. A., An introduction to cyclic voltammetry. *J. Chem. Educ.* **1983,** *60* (9), 697-702.

35. Yue, G.; Li, F.; Yang, G.; Zhang, W., Efficient Nickel Sulfide and Graphene Counter Electrodes Decorated with Silver Nanoparticles and Application in Dye-Sensitized Solar Cells. *Nanoscale Research Letters* **2016,** *11* (1), 239.

36. Adeloju, S., *Amperometry*. Elsevier Press Ltd: 2005; p pp 70-79.

37. Skoog, D. A.; Crouch, S. R.; Holler, F. J., *Principles of instrumental analysis*. Thomson Brooks/Cole: Belmont, CA, 2007.

38. E. Schirmer, R., *Modern methods of pharmaceutical analysis*. 2nd ed.; CRC Press: 1982; Vol. 1.

39. Galvao de Lima, R.; Bonato, P. S.; Santana da Silva, R., Analysis of albendazole metabolites by electrospray LC-MS/MS as a probe to elucidate electro-oxidation mechanism of albendazole. *J. Pharm. Biomed. Anal.* **2003,** *32* (2), 337-343.

40. Castro, L. S.; Kviecinski, M. R.; Ourique, F.; Parisotto, E. B.; Grinevicius, V. M.; Correia, J. F.; Wilhelm Filho, D.; Pedrosa, R. C., Albendazole as a promising molecule for tumor control. *Redox biology* **2016,** *10*, 90-99.

41. Lai, H.; Sasaki, T.; Singh, N. P., Targeted treatment of cancer with artemisinin and artemisinin-tagged iron-carrying compounds. *Expert opinion on therapeutic targets* **2005,** *9* (5), 995-1007.

42. Costa, S. F.; Weiss, L. M., Drug treatment of microsporidiosis. *Drug Resistance Updates* **2000,** *3* (6), 384-399.

43. Horton, J., Albendazole: a review of anthelmintic efficacy and safety in humans. *Parasitology* **2000,** *S121* S113-132.

44. Venkatesan, P., Albendazole. *Journal of Antimicrobial Chemotherapy* **1998,** (41), 145–147.

45. Mirfazaelian, A.; Rouini, M. R.; Dadashzadeh, S., Time dependent pharmacokinetics of albendazole in human. *Biopharm. Drug Dispos.* **2003,** *24* (5), 199-204.

46. Fraga, C. M.; Costa, T. L.; Bezerra, J. C. B.; de Souza Lino Junior, R.; Vinaud, M. C., Fatty acids oxidation and alternative energy sources detected in Taenia crassiceps cysticerci after host treatment with antihelminthic drugs. *Experimental Parasitology* **2012,** *131* (1), 111-115.

47. Li, Q.-z.; Hao, Y.-h.; Gao, X.-j.; Gao, W.-x.; Zhao, B., The Target of Benzimidazole Carbamate Against Cysticerci cellulosae. *Agricultural Sciences in China* **2007,** *6* (8), 1009-1017.

48. Jung, H.; Medina, L.; Garcia, L.; Fuentes, I.; Moreno-Esparza, R., Absorption studies of albendazole and some physicochemical properties of the drug and its metabolite albendazole sulphoxide. *J Pharm Pharmacol* **1998,** *50* (1), 43-8.

49. Virkel, G.; Imperiale, F.; Lifschitz, A.; Pis, A.; Alvarez, A.; Merino, G.; Prieto, J.; Lanusse, C., Effect of amphiphilic surfactant agents on the gastrointestinal absorption of albendazole in cattle. *Biopharm. Drug Dispos.* **2003,** *24* (3), 95-103.

50. Danaher, M.; De Ruyck, H.; Crooks, S. R.; Dowling, G.; O'Keeffe, M., Review of methodology for the determination of benzimidazole residues in biological matrices. *Journal of Chromatography B* **2007,** *845* (1), 1-37.

51. Khalil, Z.; El Karbane, M.; Faouzi, M. E. A.; Ansar, M.; Azougagh, M.; El Harti, J.; Taoufik, J., Comparative plasma disposition kinetics of albendazole and its new benzimidazol prodrug in dog. *Ann. Pharm. Fr.* **2016,** *74* (1), 21-26.

52. Perisa, M.; Babic, S., Simultaneous determination of pharmaceuticals and some of their metabolites in wastewaters by high performance liquid chromatography with tandem mass spectrometry. *J. Sep. Sci.* **2014,** *37* (11), 1289-1296.

53. Zhang, X.; Xu, H.; Zhang, H.; Guo, Y.; Dai, Z.; Chen, X., Simultaneous determination of albendazole and its metabolites in fish muscle tissue by stable isotope dilution ultra-performance liquid chromatography tandem mass spectrometry. *Anal. Bioanal. Chem.* **2011,** *401* (2), 727-734.

54. Belaz, K. R. A.; Pereira-Filho, E. R.; Oliveira, R. V., Development of achiral and chiral 2D HPLC methods for analysis of albendazole metabolites in microsomal fractions using multivariate analysis for the in vitro metabolism. *Journal of Chromatography B* **2013,** *932* (Supplement C), 26-33.

55. Wu, M.; Hu, J., Residue analysis of albendazole in watermelon and soil by solid phase extraction and HPLC. *Anal. Lett.* **2014,** *47* (2), 356-366.

56. Sibel A. Ozkan, J.-M. K., Petr Zuman, *Electroanalysis in Biomedical and Pharmaceutical Sciences*. Springer: 2015.

57. Miyano, D. M.; Lima, T.; Simoes, F. R.; La-Scalea, M. A.; Oliveira, H. P. M.; Codognoto, L., Electrochemical study of simple coumarin and its determination in aqueous infusion of Mikania glomerata. *J. Braz. Chem. Soc.* **2014,** *25* (3), 602-609.

58. Riveros, G.; Gonzalez, G.; Chornik, B., Modification of silicon surface with redox molecules derived from ferrocene. *J. Braz. Chem. Soc.* **2010,** *21* (1), 25-32.

59. Gowda, J. I.; Nandibewoor, S. T., Electrochemical behavior of paclitaxel and its determination at glassy carbon electrode. *Asian Journal of Pharmaceutical Sciences* **2014,** *9* (1), 42-49.

60. Li, C., Electrochemical determination of dipyridamole at a carbon paste electrode using cetyltrimethyl ammonium bromide as enhancing element. *Colloids and Surfaces B: Biointerfaces* **2007,** *55* (1), 77-83.

61. Meena Ashok K, S. K., Kandaswamy, Murugesh, Rajagopal, Sriram, Mullangi, Ramesh, Formulation development of an albendazole self-emulsifying drug delivery system (SEDDS) with enhanced systemic exposure / Razvoj samoemulzifirajućeg sustava za isporuku albendazola (SEDDS) s pojačanom sistemskom apsorpcijom. In *Acta Pharmaceutica*, 2012; Vol. 62, p 563.

62. Joudieh, S.; Bon, P.; Martel, B.; Skiba, M.; Lahiani-Skiba, M., Cyclodextrin polymers as efficient solubilizers of albendazole: complexation and physico-chemical characterization. *J. Nanosci. Nanotechnol.* **2009,** *9* (1), 132-140.

63. Palomares-Alonso, F.; González, C. R.; Bernad-Bernad, M. J.; Montiel, M. D. C.; Hernández, G. P.; González-Hernández, I.; Castro-Torres, N.; Estrada, E. P.; Jung-Cook, H., Two novel ternary albendazole–cyclodextrin–polymer systems: Dissolution, bioavailability and efficacy against Taenia crassiceps cysts. *Acta Tropica* **2010,** *113* (1), 56-60.

64. Pourgholami, M. H.; Wangoo, K. T.; Morris, D. L., Albendazole-cyclodextrin complex: enhanced cytotoxicity in ovarian cancer cells. *Anticancer Res.* **2008,** *28* (5A), 2775-2779.

65. Pradines, B.; Gallard, J.-F.; Iorga, B. I.; Gueutin, C.; Loiseau, P. M.; Ponchel, G.; Bouchemal, K., Investigation of the complexation of albendazole with cyclodextrins for the design of new antiparasitic formulations. *Carbohydr. Res.* **2014,** *398*, 50-55.

66. Hossein Pourgholami, M.; Yan Cai, Z.; Lu, Y.; Wang, L.; Lawson Morris, D., Albendazole: a Potent Inhibitor of Vascular Endothelial Growth Factor and Malignant Ascites Formation in OVCAR-3 Tumor-Bearing Nude Mice. *Clinical Cancer Research* **2006,** *12* (6), 1928-1935.

67. Pillai, K.; Akhter, J.; Morris, D. L., Super Aqueous Solubility of Albendazole in β-Cyclodextrin for Parenteral Application in Cancer therapy. *J Cancer* **2017,** *8* (6), 913-923.

68. Prashanth, S. N.; Ramesh, K. C.; Seetharamappa, J., Electrochemical oxidation of an immunosuppressant, mycophenolate mofetil, and its assay in pharmaceutical formulations. *Int. J. Electrochem.* **2011**, 193041, 7 pp.

69. Rezaei, B.; Damiri, S., Voltammetric behavior of multi-walled carbon nanotubes modified electrode-hexacyanoferrate(II) electrocatalyst system as a sensor for determination of captopril. *Sensors and Actuators B: Chemical* **2008,** *134* (1), 324-331.

70. Laviron, E., General expression of the linear potential sweep voltammogram in the case of diffusionless electrochemical systems. *Journal of Electroanalytical Chemistry and Interfacial Electrochemistry* **1979,** *101* (1), 19-28.

71. Fröhlich, T.; Çapcı Karagöz, A.; Reiter, C.; Tsogoeva, S. B., Artemisinin-Derived Dimers: Potent Antimalarial and Anticancer Agents. *Journal of Medicinal Chemistry* **2016,** *59* (16), 7360-7388.

72. Efferth, T.; Zacchino, S.; Georgiev, M. I.; Liu, L.; Wagner, H.; Panossian, A., Nobel Prize for artemisinin brings phytotherapy into the spotlight. *Phytomedicine* **2015,** *22* (13), A1-3.

73. O'Neill, P. M.; Barton, V. E.; Ward, S. A., The molecular mechanism of action of artemisinin - the debate continues. *Molecules* **2010,** *15*, 1705-1721.

74. Mugweru, A. M.; Shore, A.; Kahi, H. K.; Kamau, G. N., Electrochemical and Spectroscopic Characteristics of Artemisinin Antimalarial Drug: Charge Transfer Redox Process. *Int. J. Chem. Kinet.* **2016,** *48* (2), 72-78.

75. O'Neill, P. M.; Barton, V. E.; Ward, S. A., The Molecular Mechanism of Action of Artemisinin—The Debate Continues. *Molecules* **2010,** *15* (3), 1705.

76. Bray, P. G.; Ward, S. A.; O'Neill, P. M., Quinolines and artemisinin: chemistry, biology and history. *Curr. Top. Microbiol. Immunol.* **2005,** *295* (Malaria), 3-38.

77. Vamvakaki, V.; Tsagaraki, K.; Chaniotakis, N., Carbon Nanofiber-Based Glucose Biosensor. *Analytical Chemistry* **2006,** *78* (15), 5538-5542.

78. Mazzochette, Z.; Newton, E.; Mugweru, A., Electrochemical catalysis of artemisinin on hemoglobin functionalized carbon nanofibers. *Anal. Methods* **2017,** *9* (20), 2997-3002.

79. Posner, G. H.; Wang, D.; Cumming, J. N.; Oh, C. H.; French, A. N.; Bodley, A. L.; Shapiro, T. A., Further Evidence Supporting the Importance of and the Restrictions on a Carbon-Centered Radical for High Antimalarial Activity of 1,2,4-Trioxanes Like Artemisinin. *J. Med. Chem.* **1995,** *38* (13), 2273-5.

80. Tan, X.-C.; Zhang, J.-L.; Tan, S.-W.; Zhao, D.-D.; Huang, Z.-W.; Mi, Y.; Huang, Z.-Y., Amperometric Hydrogen Peroxide Biosensor Based on Immobilization of Hemoglobin on a Glassy Carbon Electrode Modified with Fe3O4/Chitosan Core-Shell Microspheres. *Sensors* **2009,** *9* (8), 6185.

81. Xian, Y.; Xian, Y.; Zhou, L.; Wu, F.; Ling, Y.; Jin, L., Encapsulation hemoglobin in ordered mesoporous silicas: Influence factors for immobilization and bioelectrochemistry. *Electrochemistry Communications* **2007,** *9* (1), 142-148.

82. Lihua, C.; Yongkang, Z.; Hong, Y.; Liuzhan, L.; Zhaoxia, Y.; Hanxi, S., Fluorescence determination of artemisinin using hemoglobin as catalyst and pyronine B as substrate. *Wuhan University Journal of Natural Sciences* **2006,** *11* (3), 704-708.